

# Generalized Bayesian Multidimensional Scaling and Model Comparison

Jiarui Zhang\* and Liangliang Wang\*

**Abstract.** Multidimensional scaling is widely used to reconstruct a map with the points' coordinates in a low-dimensional space from the original high-dimensional space while preserving the pairwise distances. In a Bayesian framework, the current approach using Markov chain Monte Carlo algorithms has limitations in terms of model generalization and performance comparison. To address these limitations, a general framework that incorporates non-Gaussian errors and robustness to fit different types of dissimilarities is developed. Then, an adaptive inference method using annealed Sequential Monte Carlo algorithm for Bayesian multidimensional scaling is proposed. This algorithm performs inference sequentially in time and provides an approximate posterior distribution over the points' coordinates in a low-dimensional space and an unbiased estimator for the marginal likelihood. In this study, we compare the performance of different models based on marginal likelihoods, which are produced as a byproduct of the adaptive annealed Sequential Monte Carlo algorithm. Using synthetic and real data, we demonstrate the effectiveness of the proposed algorithm. Our results show that the proposed algorithm outperforms other benchmark algorithms under the same computational budget based on common metrics used in the literature. The implementation of our proposed method and applications are available at <https://github.com/nunujiarui/GBMDS>.

**Keywords:** Sequential Monte Carlo, dimension reduction, adaptive inference, robustness, skewness, visualization.

## 1 Introduction

Multidimensional scaling (MDS) is a method of dimension reduction that represents objects as points in a multidimensional space using a given collection of pairwise dissimilarities between objects. In MDS, a two- or three-dimensional representation of high-dimensional data can be chosen so that the distance between points in the lower-dimensional space is similar to the distance in the original space. MDS is widely used in various fields, such as psychology, social science, genomics, etc. One use of MDS is visualization, allowing people to explore patterns in the data by creating spatial representations based on distances. By visualizing the spatial arrangement of data points, hidden patterns can be more easily identified. In the context of high-dimensional data, transforming data points into a lower-dimensional space using MDS can facilitate visualization and statistical analysis. Another practical application of MDS is data exploration, where people gain insight into the main dimensions that underlie the dissimilarities.

---

\*Department of Statistics and Actuarial Science, Simon Fraser University, Canada. [jiarui\\_zhang@sfu.ca](mailto:jiarui_zhang@sfu.ca), [lwa68@sfu.ca](mailto:lwa68@sfu.ca)

There are two primary categories of MDS techniques, namely metric and non-metric methods. In metric MDS, the dissimilarities are assumed to be numerical. It is useful when the dissimilarities follow a Euclidean geometry, and the dissimilarity matrix satisfies the metric axioms. On the other hand, nonmetric MDS is often preferred by some researchers for particular applications in which the dissimilarities between objects are of an ordinal or rank-based nature, and where the distances do not have a well-defined Euclidean interpretation. Both metric and non-metric MDS produce a configuration where high-dimensional data points are depicted as lower-dimensional points. This arrangement reflects the similarity relationships among data points. Our study primarily centers on the metric MDS methods. For a comprehensive review of modern MDS methods, refer to [Borg and Groenen \(2005\)](#).

Classical multidimensional scaling (CMDS) is a well-known dimension reduction method for metric MDS developed by [Torgerson \(1952\)](#). CMDS is effective when the given pairwise dissimilarities are precisely equal to the Euclidean distances and when the optimal low-dimensional configuration is accurately specified ([Oh and Raftery, 2001](#)). However, these assumptions can limit the performance of CMDS in some cases. Additionally, it is reasonable to assume some errors in the dissimilarities in certain situations.

[Oh and Raftery \(2001\)](#) developed a Bayesian multidimensional scaling (BMDS) method by modeling the observed dissimilarities as equal to Euclidean distances plus measurement errors. Numerical solutions of the objects' locations in the low-dimensional space are obtained via a standard Markov chain Monte Carlo (MCMC) algorithm, a commonly used variate generation technique that provides powerful tools for approximating posterior distributions. Their results indicate that the BMDS demonstrates superior accuracy in fitting certain datasets compared to the CMDS method. The performance enhancement of the BMDS method is particularly significant in cases involving notable measurement errors in data, or violations of the Euclidean assumption, or incorrect specification of the latent dimension.

The Bayesian approach to the MDS problem has become increasingly attractive due to its superior performance and flexibility in accommodating external knowledge by means of prior specification. [Oh and Raftery \(2007\)](#) integrated the BMDS framework in [Oh and Raftery \(2001\)](#) with a Bayesian model-based clustering method to achieve dimension reduction in the clustering of high-dimensional objects. [Bakker and Poole \(2013\)](#) assumed the observed distances follow a log-normal distribution and employ a standard optimization method that minimizes the squared error loss function to isolate a single Bayesian posterior that can subsequently be analyzed using standard MCMC. [Lin and Fong \(2019\)](#) implemented a  $t$ -distribution to model the objects' locations which yields a more robust estimation, and variable selection is accomplished by incorporating a latent multivariate regression structure. Regarding the advancement of the sampling algorithm for BMDS, the differential evolution MCMC algorithm is used in [Gronau and Lee \(2020\)](#) to improve sampling in standard MCMC algorithms and explore the implementation with psychologically interpretable metrics such as the Euclidean and Minkowski metrics. Hamiltonian Monte Carlo (HMC) ([Neal et al., 2011](#)) is another sampling algorithm used in [Holbrook et al. \(2020\)](#) for BMDS with applications in phylogenetics. [Holbrook et al. \(2020\)](#) also applied massive parallelization using multi-core

central processing units and graphics processing units to accelerate the computation. However, a comprehensive Bayesian modeling framework has not yet been proposed to incorporate non-Gaussian errors and extend beyond the Euclidean space for dissimilarities. Furthermore, despite the widespread utilization of the MCMC algorithms, there exist certain limitations to the methodology of Markov chains.

One problem that users face is that MCMC algorithms do not easily take advantage of highly parallel computer architectures. Additionally, a limitation shared by MCMC-based algorithms is that their marginal likelihood estimators are generally biased. To better utilize computational power and construct unbiased estimators, researchers have developed Sequential Monte Carlo (SMC) methods to compute Bayesian estimates (see [Doucet et al., 2001](#); [Doucet and Johansen, 2009](#), for an introduction to SMC). In general, SMC method uses a set of random samples called particles to approximate a sequence of probability distributions of interest ([Doucet et al., 2006](#)). It propagates the particles through time using sequential importance sampling with resampling mechanisms and provides a flexible framework for constructing unbiased estimators. One variant of SMC methods that closely resembles standard MCMC is referred to as the annealed sequential Monte Carlo (annealed SMC) algorithm ([Del Moral et al., 2006](#); [Wang et al., 2021](#)). It inherits the advantages of the SMC and can use any existing MCMC proposals. The annealed SMC also produces unbiased estimators of the marginal likelihood for free as a benefit of adopting the SMC framework. This offers a convenient way to perform model comparison using the Bayes factor ([Jeffreys, 1935](#); [Han and Carlin, 2001](#); [Zhou et al., 2016](#); [Wang et al., 2020](#)) that relies on the computation of the marginal likelihood estimates. Additionally, the annealed SMC is less likely to get stuck in local modes compared to MCMC under the same computational budget. It begins with distributions from which it is easy to sample, and then gradually increases complexity to explore the space. This gradual movement avoids getting stuck in local maxima or minima. Previous research has demonstrated the efficiency of annealing approaches in various contexts, such as epidemiology ([Del Moral et al., 2012](#)), phylogenetics ([Wang et al., 2020](#)), and solving nonlinear differential equation systems ([Wang et al., 2021](#)).

The existing BMDS methods have several limitations. First, almost all these methods are based on the Euclidean distance metric. But Euclidean dissimilarity is not always the appropriate metric in various fields. In medical imaging and 3D face recognition, the minimum-distortion mapping between two surfaces is measured by the Gromov-Hausdorff distance in [Mémoli \(2011\)](#) and the partial embedding distance in [Bronstein et al. \(2006\)](#). In text mining, the Cosine dissimilarity is often used ([Li and Han, 2013](#)), which calculates the dissimilarity between two vectors in an inner product space based on the cosine of the angle between them. The Euclidean distance may not be suitable for comparing small and large text documents, as it would be very large in this case. In contrast, the Cosine dissimilarity reflects the relative comparison of individual vectors in high dimensions regardless of magnitude, which is more suitable than the Euclidean distance. Second, the existing MDS methods mainly rely on the assumption of Gaussian errors, resulting in a lack of robustness and generality. Third, the existing literature on model comparison for BMDS frameworks with diverse dissimilarity modeling distributions is limited. The majority of previous studies have concentrated on comparing Bayesian and frequentist solutions to MDS problems by employing specific

statistics tailored for particular scenarios. Fourth, the rapid progress in data collection and storage has resulted in a vast amount of data, which poses a significant challenge for researchers seeking appropriate inference methods for handling increasingly large datasets. Bayesian inference, while known for its flexibility, is often computationally expensive. Consequently, applying Bayesian inference to MDS methods in the context of large data remains a challenging task.

To address the potential deficiencies of the current BMDS methods, we propose a more comprehensive Bayesian modeling framework, called generalized Bayesian multi-dimensional scaling (GBMDS), to incorporate general dissimilarity metrics and non-Gaussian errors into BMDS. We design an adaptive inference framework using the annealed SMC algorithm to obtain Bayesian solutions under the proposed GBMDS model. The developed algorithm does not require designing novel proposals, as in the SMC method. Instead, people can directly use the rich resources of Metropolis-Hastings proposals, making it easy to incorporate into existing MCMC approaches. Our adaptive annealed SMC algorithm considers cases where the number of observations, the dimensions of the parameters and hidden variables increase over time. The objective is to conduct sequential inferences as new data become available, allowing people to update and refine the most recent results. The proposed adaptive scheme can be readily implemented for datasets with large sample sizes through the division of data into smaller batches. The Bayesian inference can then be conducted sequentially for each batch, allowing for incremental updates.

Our contributions can be summarized as follows. i. We generalize the BMDS model to include the non-Gaussian errors in the pairwise dissimilarities. The proposed model can handle dissimilarities with heavier tails or skewed distributions and exhibit robustness and accuracy. ii. Our proposed GBMDS considers more general distance metrics that are not restricted to Euclidean space. iii. We propose a framework to perform efficient adaptive Bayesian inference for the GBMDS based on annealed SMC, which reduces the overall computational burden for large-scale data scenarios. iv. Our framework can provide unbiased estimators of the marginal likelihood as a byproduct of sampling, which makes the model comparison via the Bayes factor straightforward. v. We employ the adaptive annealed SMC in two simulation studies and three real data applications, showcasing its superior estimation capabilities compared to benchmark methods across diverse dissimilarity metrics.

The rest of this article is organized as follows. Section 2 describes the models for BMDS: we propose the GBMDS model, define the priors, and discuss model comparison and issue of identifiability in Section 2.1 to 2.4. Section 3 depicts the implementation for the GBMDS model: Sections 3.1 and 3.2 detail the initialization and inference procedure; Section 3.3 outlines the adaptive mechanism with annealed SMC algorithm. Simulations and Examples are presented in Sections 4 and 5. The conclusion is in Section 6.

## 2 BMDS Models

Suppose we have a set of  $n$  objects in the study. Let  $\mathbf{Z} = \{\mathbf{z}_1, \dots, \mathbf{z}_n\}$  be a set of observed points with  $\mathbf{z}_i = (z_{i,1}, \dots, z_{i,q})^\top \in \mathbb{R}^q$  representing the values of  $q$  attributes

in object  $i$ . The value of  $q$  is usually high, which makes the visualization of the points in their original dimension hard. Let  $\mathbf{D}$  be the matrix of dissimilarities with entry  $d_{i,j}$  as the dissimilarity between objects  $i$  and  $j$ . The dissimilarity matrix  $\mathbf{D}$  is computed from the observed data  $\mathbf{z}_1, \dots, \mathbf{z}_n$  with specific dissimilarity metrics such as Euclidean metric. Dissimilarity metrics used in this study will be detailed in Section 2.1. A formal definition of the metric space is given in *Supplementary*.

Let  $\mathbf{x}_i = (x_{i,1}, \dots, x_{i,p})^\top \in \mathbb{R}^p$  be the unobserved vector representing the values of  $p$  significant attributes in object  $i$ . The goal of MDS methods is to find the set of points  $\mathbf{X} = \{\mathbf{x}_1, \dots, \mathbf{x}_n\}$  such that  $d_{i,j}$  and  $\|\mathbf{x}_i - \mathbf{x}_j\|_p$  are as close as possible, where  $\|\cdot\|_p$  represents the  $L^p$  norm. In such a manner, the given dissimilarities are well-reproduced by the resulting configuration. We refer to this process as object configuration (Oh and Raftery, 2001), which describes the estimation of values for objects' significant attributes.

CMDS is a commonly used dimension reduction technique for metric MDS developed by Torgerson (1952). CMDS assumes the dissimilarity to be Euclidean and takes the pairwise dissimilarities as inputs and outputs the coordinates of points in a low-dimensional space up to locations, rotations and reflections. Numerical optimization techniques can be used to find a solution to the minimization problem below:

$$\min \sum_{i \neq j=1, \dots, n} (d_{i,j} - \|\mathbf{x}_i - \mathbf{x}_j\|_p)^2. \quad (1)$$

The minimizers can be expressed analytically in terms of matrix eigendecompositions when the input dissimilarities satisfy the metric inequality and can be represented by Euclidean distances. CMDS can retrieve the complete configuration of objects (up to location shift) when the dissimilarities are precisely equal to the distances in the low-dimensional space and the dimension is appropriately specified. However, the dissimilarities between observed points are usually contaminated by errors, and the underlying dimensions are often unknown.

## 2.1 Generalized Bayesian multidimensional scaling

While Euclidean distance is one of the most widely used distance measures, it is not scale-invariant, meaning that distances computed from features might be skewed depending on the units. Moreover, Euclidean distance becomes less useful as the dimensionality of the data increases. To satisfy the various needs of different tasks, we develop a general framework that can accommodate different distance metrics and behave robustly when outliers are present in the dissimilarities.

We restrict the dissimilarity measure  $d_{i,j}$  to be always positive, and assume  $d_{i,j}$  to follow some truncated distribution:

$$d_{i,j} \sim g(\delta_{i,j}) I(d_{i,j} > 0), \quad i \neq j, i, j = 1, \dots, n, \quad (2)$$

where  $I(\cdot)$  is an indicator function. The true dissimilarity measure  $\delta_{i,j}$  is modeled as the distance between object  $i$  and  $j$  using the dissimilarity metric  $\mathcal{D}$ :

$$\delta_{i,j} = \mathcal{D}(\mathbf{x}_i, \mathbf{x}_j). \quad (3)$$

The GBMDS framework we propose is general in nature. The various GBMDS models differ from one another based on the selection of dissimilarity metric  $\mathcal{D}$  and the choice of distribution function  $g$ .

Compared with the BMDS framework proposed in [Oh and Raftery \(2001\)](#), we do not restrict  $d_{i,j}$  to be accompanied by Gaussian errors. The previous BMDS framework may be inadequate when dealing with dissimilarity measures that are subject to random errors or those that are non-Euclidean in nature. In addition, the assumption of utilizing a truncated Gaussian distribution to model the errors is inadequate in the presence of outliers. The presence of outliers can lead to increased uncertainty surrounding unobserved dissimilarities ( $\delta_{i,j}$ 's) beyond what can be accounted for by the tails of Gaussian distributions. We will refer to the framework in [Oh and Raftery \(2001\)](#) as the standard BMDS throughout this paper.

### Dissimilarity metrics

The standard choice of dissimilarity metric  $\mathcal{D}$  on  $\mathbb{R}^p$  is the Euclidean metric ( $L^2$  norm):  $\mathcal{D}(\mathbf{x}_i, \mathbf{x}_j) = \|\mathbf{x}_i - \mathbf{x}_j\|_2 = \sqrt{\sum_{k=1}^p (x_{i,k} - x_{j,k})^2}$ . It is often used in MDS when the dissimilarity matrix satisfies the metric axioms and has a well-defined Euclidean interpretation.

We generalize the standard BMDS by considering cases where the dissimilarity matrix may not have a well-defined Euclidean interpretation. In this case, we can consider candidate models with non-Euclidean dissimilarity metrics. For example, Cosine metric is defined as  $\mathcal{D}(\mathbf{x}_i, \mathbf{x}_j) = 1 - (\sum_{k=1}^p x_{i,k} x_{j,k}) / \left( \sqrt{\sum_{k=1}^p x_{i,k}^2} \sqrt{\sum_{k=1}^p x_{j,k}^2} \right)$ . The Cosine metric ranges from 0 to 1. It can be used for text analysis, as word frequencies are non-negative.

In our GBMDS framework, a variety of distributions can be considered for  $g$ , including both symmetric and skewed distributions. Symmetric distributions, such as Gaussian or Student's  $t$ -distributions, are suitable in some cases, while in other scenarios, a skewed distribution is more appropriate. In what follows, we will focus on the truncated skewed Gaussian distribution. This distribution is a suitable choice when the errors are skewed. Then, we will proceed to investigate the truncated Student's  $t$ -distribution. This distribution is deemed a suitable choice for robust estimation when outliers exist.

### GBMDS with truncated skewed Gaussian distribution

We consider that some dissimilarities can be simultaneously skewed and positive. We denote the model with truncated skewed Gaussian distribution as  $\mathcal{M}_{TSN}$  and model the dissimilarity  $d_{i,j}$  as follows:

$$d_{i,j} | \mathcal{M}_{TSN} \sim \mathcal{SN}(\delta_{i,j}, \sigma^2, \psi) I(d_{i,j} > 0), \quad i \neq j, i, j = 1, \dots, n,$$

where  $\sigma^2 \in \mathbb{R}^+$  is the squared scale parameter and  $\psi \in \mathbb{R}$  is the shape parameter. The truncated Gaussian distribution is recovered when  $\psi$  is zero. As the absolute value of  $\psi$

grows, the absolute skewness of the distribution increases, with negative  $\psi$  producing a left-skewed distribution and positive  $\psi$  generating a right-skewed distribution.

For a given matrix of dissimilarities  $\mathbf{D}$ , the likelihood function,  $l$ , of the latent variables  $\mathbf{X} = \{\mathbf{x}_{1:n}\}$ , unknown parameters  $\sigma^2$  and  $\psi$  under  $\mathcal{M}_{TSN}$ , can be written as:

$$l(\mathbf{D}|\mathbf{X}, \sigma^2, \psi, \mathcal{M}_{TSN}) \propto \left\{ \sigma^2 (1 - F_{\delta_{i,j}, \sigma, \psi}(0)) \right\}^{-\frac{m}{2}} \times \exp \left\{ -\frac{1}{2\sigma^2} \text{SSR} \right\} \times \prod_{i>j} \Phi \left( \psi \frac{d_{i,j} - \delta_{i,j}}{\sigma} \right), i, j = 1, \dots, n \quad (4)$$

where  $F(\cdot)$  is the cdf of skewed Gaussian distribution,  $\text{SSR} = \sum_{i>j} (d_{i,j} - \delta_{i,j})^2$  is the sum of squared residuals,  $\Phi(\cdot)$  is the standard Gaussian cdf, and  $m = n(n-1)/2$  is the total number of dissimilarities for  $n$  objects.

### Robust GBMDS with truncated Student's $t$ -distribution

To further relax the assumption of constant Gaussian error variance in the dissimilarity, we introduce the model with truncated Student's  $t$ -distribution. Consequently, we can accommodate different degrees of uncertainty associated with dissimilarity by using different error variances. The  $t$ -distribution is often used as an alternative to the Gaussian distribution as a more robust model to fit data with heavier tails (Lange et al., 1989; Lin and Fong, 2019). In many applications, the outliers add more uncertainty around the tails of the dissimilarity measures. Fitting the truncated  $t$ -distribution provides a longer tail.

The  $t$ -distribution can be written in the form of its scale mixtures of Gaussian representation to demonstrate its robustness property:

$$t_{\text{df}}(x; \mu, \sigma^2) = \int_0^\infty \mathcal{N}\left(x; \mu, \frac{\sigma^2}{\zeta}\right) \text{Gamma}\left(\zeta, \frac{\nu}{2}, \frac{\nu}{2}\right) d\zeta. \quad (5)$$

Equation (5) indicates that if a random variable  $x$  follows a  $t$ -distribution with mean  $\mu$ , variance  $\sigma^2$ , and degrees of freedom  $\nu$ , then conditioning on  $\zeta \sim \text{Gamma}(\nu/2, \nu/2)$ ,  $x$  follows a Gaussian distribution with parameters  $\mu$  and  $\sigma^2/\zeta$ . The  $t$ -distribution down-weights the observations which are disparate from the majority under the Gaussian distribution. This means that observations that are outliers or significantly different from the majority of the data will have less influence on the overall distribution in the  $t$ -distribution compared to the Gaussian distribution.

We denote the model with truncated  $t$ -distribution as  $\mathcal{M}_T$ .  $\mathcal{M}_T$  models the dissimilarity  $d_{i,j}$  as follows:

$$\zeta_{i,j} \sim \text{Gamma}(\nu/2, \nu/2), \\ d_{i,j}|\mathcal{M}_T \sim \mathcal{N}\left(\delta_{i,j}, \sigma^2/\zeta_{i,j}\right) I(d_{i,j} > 0), \quad i \neq j, i, j = 1, \dots, n.$$

For a given matrix of dissimilarities  $\mathbf{D}$ , the likelihood function of the latent variables  $\mathbf{X} = \{\mathbf{x}_{1:n}\}$ , unknown parameters  $\sigma^2$  and  $\zeta_{i,j}$  under  $\mathcal{M}_T$ , can be written as:

$$l(\mathbf{D}|\mathbf{X}, \sigma^2, \zeta_{i,j}, \mathcal{M}_T) = (2\pi\sigma^2)^{-\frac{m}{2}} \times \exp\left\{\frac{1}{2}\sum_{i>j}\log(\zeta_{i,j}) - \frac{1}{2\sigma^2}\sum_{i>j}\zeta_{i,j}(d_{i,j} - \delta_{i,j})^2 - \sum_{i>j}\log\Phi\left(\frac{\delta_{i,j}\sqrt{\zeta_{i,j}}}{\sigma}\right)\right\}, \quad (6)$$

where SSR,  $\Phi(\cdot)$ , and  $m = n(n-1)/2$  are defined as in the model  $\mathcal{M}_{TSN}$ . The derivation of the likelihood function under the model  $\mathcal{M}_T$  is given in *Supplementary*.

## 2.2 Bayesian inference

### Prior distributions

Under the Bayesian framework, the prior distributions for the unknown parameters  $\mathbf{x}_i$ ,  $\sigma^2$ ,  $\psi$ , and  $\Lambda$  need to be specified in advance. We assume prior independence among parameters. For the prior of  $\mathbf{x}_i$ , we choose a multivariate Gaussian distribution with mean  $\mathbf{0}$  and a diagonal covariance matrix  $\Lambda = \text{diag}(\lambda_1, \dots, \lambda_p)$ . In other words,  $\mathbf{x}_i \sim \mathcal{N}(\mathbf{0}, \Lambda)$ , independently for  $i = 1, \dots, n$ . For the elements along the diagonal covariance matrix, we assume an inverse Gamma distribution for the hyperprior distribution, i.e.,  $\lambda_k \sim \mathcal{IG}(\alpha, \beta_k)$ , independently for  $k = 1, \dots, p$ . For  $\sigma^2$ , we use an inverse Gamma distribution for the prior distribution, i.e.,  $\sigma^2 \sim \mathcal{IG}(a, b)$ . For  $\psi$ , we choose a diffuse prior, i.e.,  $\psi \sim \mathcal{U}(c, d)$ . We denote the prior distributions of the unknown parameters as  $\pi(\mathbf{X})$ ,  $\pi(\sigma^2)$ ,  $\pi(\psi)$  and  $\pi(\Lambda)$ .

We use the same settings for the prior distributions of the unknown parameters  $\mathbf{x}_i$  and  $\sigma^2$  as in the model  $\mathcal{M}_{TSN}$ . In addition, under the setting of model  $\mathcal{M}_T$ , we use *Gamma* ( $\nu/2, \nu/2$ ) as the prior distribution for  $\zeta_{i,j}$ .

### Posterior distributions

For simplicity, we introduce a new notation  $\mathbf{s}$  to represent all the latent variables  $\mathbf{X}$  and the unknown parameters  $\boldsymbol{\theta}$ . Note that the parameters  $\boldsymbol{\theta}$  vary across different models. In the model with truncated skewed Gaussian distribution,  $\boldsymbol{\theta}$  includes  $\sigma^2$ ,  $\Lambda$ , and  $\psi$ . In the model with truncated Student's  $t$ -distribution,  $\boldsymbol{\theta}$  includes  $\sigma^2$ ,  $\Lambda$ ,  $\psi$ , and  $\zeta$ .

In the Bayesian framework, our interest is the posterior distribution on  $\mathbf{s}$  given dissimilarity matrix  $\mathbf{D}$ , denoted as:

$$\pi(\mathbf{s}|\mathbf{D}) = \frac{\gamma(\mathbf{s}|\mathbf{D})}{Z} \propto l(\mathbf{D}|\mathbf{s}) \times \pi(\mathbf{s}), \quad (7)$$

where  $\gamma(\mathbf{s}|\mathbf{D})$  denotes the unnormalized posterior distribution,  $l(\mathbf{D}|\mathbf{s})$  is the likelihood function,  $\pi(\mathbf{s})$  is the prior on the parameters, and  $Z = \int \gamma(\mathbf{s}|\mathbf{D})d\mathbf{s}$  is the marginal likelihood.



The likelihood functions are specified in Equations 4 and 6 for  $\mathcal{M}_{TSN}$  and  $\mathcal{M}_T$ , respectively. The prior distributions are described in the previous subsection. Since the normalizing constant  $Z$  is intractable, we will use Monte Carlo methods to approximate the posterior distributions, which will be detailed in Section 3.

### Adaptive Bayesian inference

Let  $\mathbf{X}^{(0)}$  be the hidden variables that are associated with objects  $\mathbf{Z}^{(0)} = \{\mathbf{z}_1, \dots, \mathbf{z}_{n_0}\}$ , and  $\mathbf{X}^{(1)}$  be the hidden variables associated with objects  $\mathbf{Z}^{(1)} = \{\mathbf{z}_{n_0+1}, \dots, \mathbf{z}_{n_0+n_1}\}$ . Given dissimilarity metric  $\mathcal{D}$ , dissimilarities  $\mathbf{D}^{(0)}$  is obtained from  $\mathbf{Z}^{(0)}$  and  $\mathbf{D}$  is obtained from  $\mathbf{Z} = (\mathbf{Z}^{(0)}, \mathbf{Z}^{(1)})$ .

In this case,  $\mathbf{s}$  is composed of three parts,  $\mathbf{X}^{(0)}$ ,  $\mathbf{X}^{(1)}$ , and  $\boldsymbol{\theta}$ . The posterior distribution of  $\mathbf{s}$  can be rewritten as:

$$\pi(\mathbf{X}^{(0)}, \mathbf{X}^{(1)}, \boldsymbol{\theta} | \mathbf{D}) \propto l(\mathbf{D} | \mathbf{X}^{(0)}, \mathbf{X}^{(1)}, \boldsymbol{\theta}) \pi(\mathbf{X}^{(0)}) \pi(\mathbf{X}^{(1)}) \pi(\boldsymbol{\theta}). \quad (8)$$

The adaptive Bayesian inference concerns the inference of  $\pi(\mathbf{X}^{(0)}, \mathbf{X}^{(1)}, \boldsymbol{\theta} | \mathbf{D})$  using the previous inference for  $\pi(\mathbf{X}^{(0)}, \boldsymbol{\theta} | \mathbf{D}^{(0)})$  when dissimilarity data increase from  $\mathbf{D}^{(0)}$  to  $\mathbf{D}$ .

When the previous dissimilarity matrix  $\mathbf{D}^{(0)}$  is not available, we denote  $\mathbf{D}^{(0)} = \emptyset$  and  $\mathbf{X}^{(0)} = \emptyset$ . With our notation, the posterior distribution in Equation 7 is a special case of Equation 8 when  $\mathbf{D}^{(0)} = \emptyset$ ,  $\mathbf{X}^{(0)} = \emptyset$ . Therefore, we will only focus on the adaptive Bayesian inference with Monte Carlo methods for Equation 8 in Section 3.

We propose to conduct adaptive Bayesian inference in two scenarios. First, in the problem of online inference, we attempt to make inference sequentially in time as data arrive or people have additional observations to update the recent results. We refer to such situations as adaptive inferences, where we are concerned with the re-computation of results that are only marginally different from those of a previously solved inference problem. The main idea is to use posteriors from the previous iteration to initialize the next iteration. The same idea also applies to the situation where the sample size of the data is significant. Instead of running the algorithm with a fixed dimension on all observations at one time, we can split the data into several batches and make inferences sequentially. We expect this is helpful in the Bayesian multidimensional scaling context as the visualization of the object can be created sequentially, which can alleviate the computational loads.

## 2.3 Model comparison

As described in the previous section, the function  $g$  can take different forms. In most cases, the optimal form of  $g$ , the number of significant attributes  $p$  or the applied dissimilarity metrics are unknown. In this section, we approach the problem of comparing a discrete set of Bayesian models with the Bayes factor. Consider two models  $\mathcal{M}_1$  and  $\mathcal{M}_2$  with different likelihoods and corresponding sets of parameters  $\mathbf{s}_1$  and  $\mathbf{s}_2$ . In the context of this paper,  $\mathcal{M}_1$  and  $\mathcal{M}_2$  would correspond to two competing models. Examples of competing models could be  $\mathcal{M}_{TSN}$  versus  $\mathcal{M}_T$ , or one model under a different

choice of dimension  $p$ . The Bayes factor is defined as the ratio of the posterior odds to the prior odds:

$$\text{Bayes Factor } (\mathcal{M}_1, \mathcal{M}_2) = \frac{P(\mathcal{M}_1|\mathbf{D})/P(\mathcal{M}_2|\mathbf{D})}{P(\mathcal{M}_1)/P(\mathcal{M}_2)}.$$

When the two models have equal prior probability, i.e.,  $P(\mathcal{M}_1) = P(\mathcal{M}_2)$ , the Bayes Factor reduces to the ratio of two marginal likelihood estimates, and is given by:

$$\text{Bayes Factor } (\mathcal{M}_1, \mathcal{M}_2) = \frac{\int P(\mathbf{s}_1|\mathcal{M}_1)P(\mathbf{D}|\mathbf{s}_1, \mathcal{M}_1) d\mathbf{s}_1}{\int P(\mathbf{s}_2|\mathcal{M}_2)P(\mathbf{D}|\mathbf{s}_2, \mathcal{M}_2) d\mathbf{s}_2} = \frac{P(\mathbf{D}|\mathcal{M}_1)}{P(\mathbf{D}|\mathcal{M}_2)}.$$

Bayes factor can provide support to either model; a Bayes factor greater than 1 indicates support for model 1 over model 2 and vice versa. A rule of thumb, as suggested in [Kass and Raftery \(1995\)](#), can be viewed as guidelines for model selection from a Bayes factor. A typical challenge for using the Bayes factor is the computation of the marginal likelihood estimates, especially for MCMC-based methods ([Wang et al., 2020](#)). Marginal likelihood estimation is not straightforward in MCMC-based methods, and additional sampling procedures are needed to obtain these estimates. Several methods have been proposed to address this issue ([Chib and Jeliazkov, 2001](#); [Skilling, 2004](#); [Robert and Wraith, 2009](#)), but each has its drawback. One additional limitation shared by all MCMC-based marginal likelihood estimators is that they are generally biased.

There are several reasons for using the Bayesian approach for model selection over the classical tools, such as  $p$ -values and some information criteria. First, the interpretation of Bayes factors is straightforward. The posterior model probabilities can be directly interpreted as probabilities that are readily understandable by even non-statisticians. Second, Bayesian model selection is consistent, while some classical model selection tools do not guarantee consistency. Moreover, as shown in [Berk \(1966\)](#), Bayesian model selection will pick the model with the closest Kullback-Leibler divergence to the true model (asymptotically and under mild conditions). Third, Bayesian model selection naturally penalizes complex models and favours simpler models when the data provides roughly comparable fits. For more discussion and references, see [Berger et al. \(2001\)](#) and [Robert et al. \(2007\)](#).

On the other side, in the frequentist view, STRESS is a commonly used measure of fit for the object configuration problem ([Kruskal, 1964](#)). STRESS value is defined as

$$\text{STRESS} = \sqrt{\frac{\sum_{i>j} (d_{i,j} - \hat{\delta}_{i,j})^2}{\sum_{i>j} d_{i,j}^2}},$$

where  $\hat{\delta}_{i,j}$  is the distance found from the estimated object configuration. MDS methods form an object configuration that minimizes the STRESS values. A smaller STRESS value indicates a better fit.

In this work, we will select the optimal Bayesian model and dimension  $p$  using the marginal likelihood estimates. We will compare and evaluate the performances of CMDs and GBMDs using the STRESS value.

## 2.4 Identifiability in multidimensional scaling

Similar to other dimensional reduction methods, identification issues exist in the posterior inference of GBMDS. For instance, the center and direction of the estimated points can be arbitrary. Given this identification issue, we propose the following way to display the uncertainty measures: We apply the Procrustes transformations (Goodall, 1991) as a standardization process on all the posterior samples of  $\mathbf{x}_i$ 's. This transformation aligns configurations with a least-squares criterion by a combination of scaling, rotation, reflection and translation. The credible regions are then constructed from the posterior samples of  $\mathbf{x}_i$ 's after this Procrustes transformation for measures of uncertainty.

# 3 Adaptive Bayesian Inference using Annealed SMC

## 3.1 Intermediate distributions and particle initialization

To conduct the Bayesian inference for the posterior distribution in Equation 8, we propose to design an artificial sequence of annealing intermediate target distributions following the ideas from the SMC literature (Neal, 2001; Del Moral et al., 2006, 2007; Wang et al., 2020). Specifically, we create a sequence of annealing intermediate target distributions  $\{\pi_r(\mathbf{s})\}_{0 \leq r \leq R}$ , such that

$$\pi_r(\mathbf{s}) \propto \gamma_r(\mathbf{s}) = \left( l(\mathbf{D}|\mathbf{s}) \pi(\mathbf{s}) \right)^{\tau_r} \times \tilde{\pi}_0(\mathbf{s})^{1-\tau_r}, \quad (9)$$

where  $\tilde{\pi}_0(\mathbf{s})$  is a *reference distribution* that is generally easy to sample from (Fan et al., 2011), and  $0 = \tau_0 < \tau_1 < \dots < \tau_R = 1$  is a sequence of annealing parameters. If  $\tau_r$  is zero, the distribution becomes the reference distribution  $\tilde{\pi}_0(\mathbf{s})$ . At the other extreme, the distribution is the posterior distribution of interest when the power  $\tau_r$  equals 1.

In our model,  $\mathbf{s}$  is a vector of all the variables in  $\mathbf{X}^{(0)}$ ,  $\mathbf{X}^{(1)}$ , and  $\boldsymbol{\theta}$ . The reference distribution can be specified for  $\mathbf{X}^{(0)}$ ,  $\mathbf{X}^{(1)}$  and  $\boldsymbol{\theta}$  independently:

$$\tilde{\pi}_0(\mathbf{s}) = \tilde{\pi}_0(\mathbf{X}^{(0)}) \tilde{\pi}_1(\mathbf{X}^{(1)}) \tilde{\pi}_0(\boldsymbol{\theta}). \quad (10)$$

Preferably, the reference distributions should possess properties that allow for convenient sampling and proximity to the modes of the target distribution. For simplicity, we choose the reference distribution for  $\boldsymbol{\theta}$  to be its prior distribution, i.e.  $\tilde{\pi}_0(\boldsymbol{\theta}) = \pi(\boldsymbol{\theta})$ , and the reference distributions for  $\mathbf{X}^{(1)}$  to be its prior,  $\tilde{\pi}_1(\mathbf{X}^{(1)}) = \pi(\mathbf{X}^{(1)})$ ; the reference distributions for  $\mathbf{X}^{(0)}$ , denoted  $\tilde{\pi}_0(\mathbf{X}^{(0)})$ , is set to be a Gaussian distribution.

With a small value of  $\tau_r$ , the intermediate target distribution is closer to the reference distribution. For parameters that rely on the prior distribution as the reference distribution, smaller  $\tau_r$  can result in flatter intermediate target distributions that facilitate the movement between various modes. The samples are coerced into the posterior distribution as we slowly increase the annealing parameter  $\tau_r$ . The initialization of particles is summarized in Algorithm 1.

---

**Algorithm 1: Particle\_Initialization**


---

**Input** : (a) Dissimilarity:  $\mathbf{D}^{(0)}, \mathbf{D}$ ; (b) Priors and reference distributions over  $\{\mathbf{x}_{1:n}\}$  and model parameters  $\boldsymbol{\theta} = \{\sigma^2, \Lambda, \psi, \zeta\}$ ; (c) Number of particles:  $K$ .  
**Output**: Initializations of  $K$  particles:  $\{\mathbf{s}_{0,k}\}_{k=1}^K$ .

```

1 for  $k \in \{1, 2, \dots, K\}$  do
2   if  $D^{(0)} \neq \emptyset$  then
3     Initialize particles of  $\mathbf{X}_{0,k}^{(0)} \sim \tilde{\pi}_0(\mathbf{X}^{(0)})$ .
4     Initialize particles of  $\mathbf{X}_{0,k}^{(1)} \sim \tilde{\pi}_1(\mathbf{X}^{(1)})$ .
5     Initialize particles of parameters with independent samples from prior distributions:
        $\{\sigma_{0,k}^2, \Lambda_{0,k}, \psi_{0,k}, \zeta_{0,k}\} \sim \pi(\boldsymbol{\theta})$ .

```

---

### 3.2 Annealed SMC

Next, we will introduce in Algorithm 2 the annealed SMC algorithm along with the adaptive mechanism for choosing the annealing sequence. The annealed SMC algorithm approximates the posterior distribution  $\pi(\mathbf{s}|\mathbf{D})$  in  $R$  steps. At each step  $r$ , we approximate  $\pi_r(\cdot)$  using a total of  $K$  particles. Each particle  $\mathbf{s}_{r,k}$  is associated with a positive weight. Let  $w_{r,k}$  denote the unnormalized weight for particle  $\mathbf{s}_{r,k}$  and let  $W_{r,k}$  denote the corresponding normalized weight. The normalization is performed by  $W_{r,k} = w_{r,k} / \sum_{k=1}^K w_{r,k}$ .

We start by sampling initial particles from the reference distributions. Then, the annealed SMC algorithm iterates between *reweighting*, *propagating*, and *resampling*. The details of the three steps in the annealed SMC algorithm are given as follows.

#### Step 1. Weight Update

The incremental importance weight for particle  $k$  at iteration  $r$  is

$$\tilde{w}_{r,k} = \frac{\gamma_r(\mathbf{s}_{r,k}) \times \kappa^-(\mathbf{s}_{r,k}, \mathbf{s}_{r-1,k})}{\gamma_{r-1}(\mathbf{s}_{r-1,k}) \times \kappa^+(\mathbf{s}_{r-1,k}, \mathbf{s}_{r,k})}, \quad (11)$$

where the forward kernel  $\kappa^+(\mathbf{s}_{r-1,k}, \mathbf{s}_{r,k})$  is a  $\pi_r$ -invariant Metropolis-Hastings kernel, and  $\kappa^-(\mathbf{s}_{r,k}, \mathbf{s}_{r-1,k})$  is the backward kernel (Del Moral et al., 2006). The selection of the backward kernel is crucial as it will affect the variance of the normalized weights. A convenient backward kernel that allows easy computation of the weight is

$$\kappa^-(\mathbf{s}_{r,k}, \mathbf{s}_{r-1,k}) = \frac{\gamma_r(\mathbf{s}_{r-1,k}) \times \kappa^+(\mathbf{s}_{r-1,k}, \mathbf{s}_{r,k})}{\gamma_r(\mathbf{s}_{r,k})}. \quad (12)$$

This approach simplifies the evaluation of weights since we do not need point-wise evaluations of the backward and forward kernels. The incremental importance weight becomes

$$\tilde{w}_{r,k} = \left[ \frac{l(\mathbf{D}|\mathbf{s}_{r-1,k}) \pi(\mathbf{s}_{r-1,k})}{\tilde{\pi}_0(\mathbf{s}_{r-1,k})} \right]^{\tau_r - \tau_{r-1}}. \quad (13)$$

The weight update function for particles at iteration  $r$  is

$$W_{r,k} \propto w_{r,k} = w_{r-1,k} \tilde{w}_{r,k}.$$

Note the weight update function only depends on the particles at the previous iteration. This is implemented in Line 9 of Algorithm 2.

*Step 2. Particle Propagation*

We sample the new particles  $\mathbf{s}_{r,k}$  from  $\pi_r$ -invariant Metropolis-Hastings kernels. The annealed SMC algorithm can directly make use of the MCMC proposals in the particle propagation. The full conditional distributions for parameters  $\lambda_j$ ,  $\{\mathbf{x}_{1:n}\}$ ,  $\sigma^2$ ,  $\psi$ , and  $\zeta_{i,j}$  are presented below. In each conditional posterior distribution, we use  $|\cdots$  to denote conditioning on the data and all other parameters and/or indicators. A detailed description of sampling methods is given in *Supplementary*.

The full conditional distribution for  $\lambda_k$  is

$$\lambda_k | \cdots \sim IG(\alpha + n/2, \beta_k + \tau_r s_k/2), \quad (14)$$

where  $s_k/n$  is the sample variance of the  $k$ th coordinates of  $\mathbf{x}_i$ 's.

The full conditional posterior distributions of  $\{\mathbf{x}_{1:n}\}$ ,  $\sigma^2$  and  $\psi$  do not admit closed forms, a random walk Metropolis-Hastings step is implemented with the Gaussian proposal densities.

For  $\mathcal{M}_{TSN}$ ,

$$\begin{aligned} \gamma_r(\{\mathbf{x}_{1:n}\} | \cdots, \mathcal{M}_{TSN}) &\propto \exp \left\{ -\tau_r \left( A + \frac{1}{2} \sum_{i=1}^n \mathbf{x}_i^\top \Lambda^{-1} \mathbf{x}_i \right) \right\}, \\ \gamma_r(\sigma^2 | \cdots, \mathcal{M}_{TSN}) &\propto \sigma^{-2(a+1)} \exp \left\{ -\tau_r \left( A + \frac{b}{\sigma^2} \right) \right\}, \end{aligned}$$

where  $A = \frac{1}{2\sigma^2} \text{SSR} + \frac{m}{2} \log \left( \sigma^2 (1 - F_{\delta_{i,j}, \sigma, \psi}(0)) \right) - \sum_{i>j} \log \left( \Phi \left( \psi \frac{d_{i,j} - \delta_{i,j}}{\sigma} \right) \right)$ .

For  $\mathcal{M}_T$ ,

$$\begin{aligned} \gamma_r(\{\mathbf{x}_{1:n}\} | \cdots, \mathcal{M}_T) &\propto \exp \left\{ -\tau_r \left( C + \frac{1}{2} \sum_{i=1}^n \mathbf{x}_i^\top \Lambda^{-1} \mathbf{x}_i \right) \right\}, \\ \gamma_r(\sigma^2 | \cdots, \mathcal{M}_T) &\propto \sigma^{-m} \exp \left\{ -\tau_r \left( C + \frac{b}{\sigma^2} \right) \right\}, \end{aligned}$$

where  $C = \frac{1}{2\sigma^2} \sum_{i>j} \zeta_{i,j} (d_{i,j} - \delta_{i,j})^2 + \sum_{i>j} \log \Phi \left( \frac{\delta_{i,j} \sqrt{\zeta_{i,j}}}{\sigma} \right)$ .

For model  $\mathcal{M}_T$ , the full conditional distribution for  $\zeta_{i,j}$  is

$$\zeta_{i,j} | \cdots, \mathcal{M}_T \sim \text{Gamma}((\tau_r + \nu)/2, \tau_r (d_{i,j} - \delta_{i,j})^2 / (2\sigma^2) + \nu/4). \quad (15)$$

### Step 3. Particle Resampling

To alleviate the issue that all normalized weights converge to 0 except for one particle in sequential importance sampling, we prune particles of low weights when the population becomes too unbalanced. Popular resampling schemes include, but are not limited to, multinomial resampling, systematic resampling, stratified resampling, and residual resampling (Douc and Cappé, 2005). For simplicity, we will use multinomial resampling in our implementation.

Resampling at each iteration will increase the variance of the importance weights. Therefore, the resampling step is performed only when the degeneracy of the particles reaches some threshold  $\epsilon$ . At each iteration  $r$ , we monitor the degeneracy of particles using the effective sampling size (ESS) (Kong, 1992):

$$\text{ESS} = \frac{1}{\sum_{k=1}^K (W_{r,k})^2}. \quad (16)$$

The relative effective sample size (rESS) normalizes the ESS between zero and one. The rESS at iteration  $r$  can be calculated by  $\text{rESS} = \text{ESS}/K$ .

The annealed SMC algorithm produces a set of particles. After the extra resampling step in the end, the output of the annealed SMC algorithm contains a list of  $K$  particles with equal weight. These particles can be used for the posterior approximation and for constructing the visualization in the lower dimensional space. To find the Bayesian estimate of  $\mathbf{X}$ , we take an approximate posterior mode of  $\{\mathbf{x}_{1:n}\}$  as described in Oh and Raftery (2001). Oh and Raftery (2001) observed that the term involving  $SSR$  dominates the posterior density. Thus, the approximate posterior mode can be found by the values of  $\{\mathbf{x}_{1:n}\}$  that minimizes  $SSR$  among all  $K$  particles. The approximate posterior mode retrieves the relative positions of  $\{\mathbf{x}_{1:n}\}$ , and they can be considered as the solution to the object configuration. Meaningful absolute positions of  $\mathbf{X}$  may be obtained from some suitable transformation defined by the users if needed.

Some challenges with MCMC-based approximations arise in the context of model comparison via marginal likelihood estimators as discussed in 2.3. Additional costs of separately estimating the marginal likelihood with some complicated formulas are needed in MCMC-based algorithms. By contrast, model selection can be accomplished effortlessly by the Bayes factor in the proposed annealed SMC algorithm. When resampling is not conducted at every step, the estimated marginal likelihood could be evaluated during the sampling process with the following formula:

$$\hat{Z}_R = \prod_{r=1}^R \sum_{k=1}^K W_{r-1,k} \tilde{w}_{r,k}.$$

Moreover, the estimates are unbiased when the annealing sequence is fixed. Past work has shown the advantages of SMC over MCMC in the context of model comparison via marginal likelihood estimators (Del Moral, 2004; Del Moral et al., 2006; Doucet and Johansen, 2009).

---

**Algorithm 2: Annealed\_SMC**


---

**Input** : (a) Initialization of  $K$  particles:  $\{\mathbf{s}_{0,k}\}_{k=1}^K$ ; (b) Priors and reference distributions over model parameters  $\mathbf{s} = \{\{\mathbf{x}_{1:n}\}, \sigma^2, \Lambda, \psi, \zeta\}$ ; (c) Likelihood function  $l(\mathbf{D}|\mathbf{s})$ ; (d) rCESS threshold  $\phi$ ; (e) Resampling threshold  $\epsilon$ .

**Output**: (a) Particle population:  $\{\mathbf{s}_{R,k}, W_{R,k}\}_{k=1}^K$ ; (b) Marginal likelihood estimates:  $\hat{Z}_R$ ; (c) Total SMC iterations:  $R$ ; (d) Sequence of annealing parameter:  $\{\tau_r\}_{r=0}^R$ .

- 1 Initialize SMC iteration index:  $r \leftarrow 1$ , initialize annealing parameter:  $\tau_0 \leftarrow 0$ , initialize marginal likelihood estimate:  $\hat{Z}_0 \leftarrow 1$ , load initial particles  $\{\mathbf{s}_{0,k}\}_{k=1}^K$ .
- 2 **for**  $k \in \{1, 2, \dots, K\}$  **do**
- 3      $w_{r,k} = 1, W_{r,k} = 1/K$ .
- 4 **for**  $r \in \{2, 3, \dots\}$  **do**
- 5     **for**  $k \in \{1, 2, \dots, K\}$  **do**
- 6         Compute incremental importance weights:  $\tilde{w}_{r,k} = \left[ \frac{l(\mathbf{D}|\mathbf{s}_{r-1,k})\pi(\mathbf{s}_{r-1,k})}{\tilde{\pi}(\mathbf{s}_{r-1,k})} \right]^{\tau - \tau_{r-1}}$ .
- 7         Determine the next annealing parameter  $\tau_r$  using bisection method with:  
            $f(\tau) = \text{rCESS}_r(W_{r-1,\cdot}, w_{r,\cdot}) = \phi$ .
- 8         **for**  $k \in \{1, 2, \dots, K\}$  **do**
- 9             Compute pre-resampling unnormalized weights:  $w_{r,k} = w_{r-1,k} \times \tilde{w}_{r,k}$ .
- 10            Normalize weights:  $W_{r,k} = w_{r,k} / (\sum_{k=1}^K w_{r,k})$ .
- 11            Sample particles  $\mathbf{s}_{r,k}$  from  $\pi_r$ -invariant Metropolis-Hastings kernels.
- 12         Update marginal likelihood estimates  $\hat{Z}_r = \hat{Z}_{r-1} \times \sum_{k=1}^K W_{r-1,k} \tilde{w}_{r,k}$ .
- 13         **if**  $\tau_r = 1$  **then**
- 14             The total number of SMC iterations  $R \leftarrow r$ .
- 15             return  $R, \{\tau_r\}_{r=0}^R, \{\mathbf{s}_{R,k}, W_{R,k}\}_{k=1}^K$ , and  $\hat{Z}_R$ ,
- 16         **else**
- 17             **if** *particle degeneracy is too severe, i.e. rESS <  $\epsilon$*  **then**
- 18                 Resample the particles, denoted  $\{\mathbf{s}_{r,k}\}_{k=1}^K$ ;
- 19                 Reset particle weights:  $w_{r,k} = 1, W_{r,k} = 1/K$ .

---

The sequence of intermediate target distributions, as defined in Equation 9, is determined by choice of the annealing sequence,  $\{\tau_r\}$ . Proper selection of the sequence of annealing parameters is one challenge in the annealed SMC. A large number of annealing parameters can improve the performance but increase the computational cost. In order to ensure the proposed particles from the current iteration can effectively approximate the subsequent intermediate target distribution, it is necessary to transition smoothly from the reference distribution ( $\tau_0 = 0$ ) to the posterior distribution ( $\tau_R = 1$ ).

We apply the adaptive annealing parameter scheme discussed in Wang et al. (2020). The main idea is to select an annealing parameter  $\tau$  such that we achieve a controlled increase in particle degeneracy. The particle degeneracy between two successive intermediate distributions is measured by the relative conditional effective sample size (rCESS) (Zhou et al., 2016),

$$\text{rCESS}_r(W_{r-1,\cdot}, \tilde{w}_{r,\cdot}) = \frac{\left(\sum_{k=1}^K W_{r-1,k} \tilde{w}_{r,k}\right)^2}{\sum_{k=1}^K W_{r-1,k} (\tilde{w}_{r,k})^2}. \quad (17)$$

Values of rCESS range from  $1/K$  to 1. With the  $\tilde{w}_{r,k}$  in Equation 13,  $\text{rCESS}_r$  is a decreasing function of  $\tau_r$ , where  $\tau_r \in (\tau_{r-1}, 1]$ . The value of rCESS over iterations is controlled by choosing the annealing parameter  $\tau$  such that

$$f(\tau) = \text{rCESS}_r(W_{r-1,\cdot}, \tilde{w}_{r,\cdot}) = \phi, \quad (18)$$

where  $\phi \in (0, 1)$  is a tuning parameter that controls the length of the sequence  $\tau_r$ . Since there exists no closed-form solution for  $\tau$  by solving  $f(\tau) = \phi$ , a bisection method is used to solve this one-dimensional search problem. The search interval is  $\tau_r \in (\tau_{r-1}, 1]$ . Given that  $f$  is a continuous function with  $f(\tau_{r-1}) - \phi > 0$  and  $f(1) - \phi < 0$  (otherwise set  $\tau_r = 1$ ), it follows that there must exist an intermediate point  $\tau^*$  with  $f(\tau^*) = \phi$ . This is implemented in Line 7 of Algorithm 2.

### 3.3 Adaptive mechanism

In the previous subsection, we presented the annealed SMC algorithm for a fixed dimension. In this section, we will describe an adaptive mechanism to enable the annealed SMC algorithm to handle increasing dimensions. The complete algorithm is presented in Algorithm 3.

Inferences are made sequentially for each batch of observations. When a new batch is available, the dissimilarity matrix  $\mathbf{D} = \{\mathbf{D}^{(0)}, \mathbf{D}^{(1)}\}$  is calculated based on all the old observations and the incremental observations. The primary objective is to conduct inference for  $\pi(\mathbf{X}^{(0)}, \mathbf{X}^{(1)}, \boldsymbol{\theta} | \mathbf{D})$ . In order to achieve this objective, we employ the strategy detailed in Section 3.1 for initializing the particles of  $\mathbf{s} = \{\mathbf{X}^{(0)}, \mathbf{X}^{(1)}, \boldsymbol{\theta}\}$ .

When previous estimations are unavailable, i.e.,  $\mathbf{D}^{(0)} = \emptyset$ ,  $\mathbf{X}^{(0)} = \emptyset$ , the reference distribution for  $\mathbf{X}^{(1)} = \mathbf{x}_{1:n}$  is based on the results from fitting CMDS:

$$\mathbf{x}_i \sim \mathcal{N}\left(\mathbf{x}_i^{\text{CMDS}}, 0.01\mathbf{I}\right), \text{ independently for } i = 1, \dots, n,$$



where  $\mathbf{x}_i^{\text{CMDS}}$  is the result from fitting CMDS on  $\mathbf{D}^{(1)}$ . The variance of the reference distribution is selected in a manner that induces the particles to concentrate around the CMDS outputs. With a small value of the annealing parameter  $\tau_r$ , the intermediate target distribution is closer to the reference distribution, which is concentrated around the CMDS outputs for  $\mathbf{D}^{(1)}$ .

When  $\mathbf{D}^{(0)} \neq \emptyset$  and  $\mathbf{X}^{(0)} \neq \emptyset$ , we choose the reference distribution to be a particle approximation to the posterior distribution of  $\mathbf{X}^{(0)}$  given  $\mathbf{D}^{(0)}$ . The reference distribution for  $\mathbf{X}^{(0)} = \mathbf{x}_{1:n_0}$  is based on the results from all particles:

$$\mathbf{x}_i \sim \mathcal{N}(\hat{\mathbf{x}}_i, \hat{\Sigma}), \text{ independently for } i = 1, \dots, n_0,$$

where  $\hat{\mathbf{x}}_i$  is the particles' posterior mode and  $\hat{\Sigma}$  is the estimated covariance matrix of all observations' particles' posterior modes from the previous computation. For the new incremental set  $\mathbf{X}^{(1)}$  in  $\mathbf{s}$ , we sample initial particles from the reference distribution, which is selected as its prior distribution for simplicity. This completes the specifications of the reference distributions in Algorithm 1. Initialization of particles is implemented from Line 3 to Line 9 of Algorithm 3.

As an example, suppose we already obtain the posterior samples of  $\mathbf{X}^{(0)}$  from  $n_0$  old observations by running the annealed SMC algorithm, and an extra of  $n_1$  new observations become available. In that case, instead of running the annealed SMC algorithm from scratch using  $n = n_0 + n_1$  observations, we can utilize the information from the posterior samples of  $\mathbf{X}^{(0)}$  to initialize values for the old observations, and use the prior distribution to initialize samples for the new observations  $\mathbf{X}^{(1)}$ . One example that illustrates the case details with incremental dimensions is given in Section 5.1.

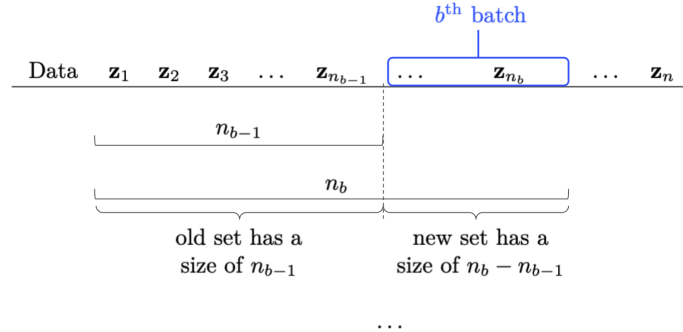


Figure 1: An illustration of the batch split.

In general, we can consider splitting data into  $B$  batches; each batch has a size of  $n_b - n_{b-1}$ , for  $b = 1, \dots, B$ , with  $n_0 = 0$ . Figure 1 illustrates the setup for the adaptive mechanism when  $b^{\text{th}}$  batch of data with size  $n_b - n_{b-1}$  is observed after the posterior samples of  $n_{b-1}$  old observations are obtained. Each batch is proceeded sequentially as outlined in Algorithm 3.

---

**Algorithm 3: Adaptive\_Annealed\_SMC**


---

**Input** : (a) Number of batches:  $B$ ; (b) Data:  $\mathbf{Z} = \{\mathbf{z}_1, \dots, \mathbf{z}_n\}$ ; (c) Dissimilarity metric:  $\mathcal{D}$ .  
**Output**: (a) Marginal likelihood estimates  $\hat{Z}_R$ ; (b) Posterior approximation,  
 $\hat{\pi}(\mathbf{s}) = \sum_{k=1}^K W_{R,k} \times \delta_{\mathbf{s}_{R,k}}(\mathbf{s})$ .

```

1 for  $b \in \{1, 2, \dots, B\}$  do
2   Calculate dissimilarities  $\mathbf{D}$  from  $\mathbf{z}_{1:n_b}$  with a given dissimilarity metric  $\mathcal{D}$ .
3   if  $b = 1$  then
4     Set both  $\mathbf{D}^{(0)}$  and  $\tilde{\pi}_0(\cdot)$  to  $\emptyset$ .
5     Set  $\tilde{\pi}_1(\mathbf{x}_i)$  to  $\mathcal{N}(\mathbf{x}_i | \mathbf{x}_i^{\text{CMDS}}, 0.01\mathbf{I})$  for  $i = 1, \dots, n_1$ .
6   else
7     Set  $\tilde{\pi}_0(\mathbf{x}_i)$  to  $\mathcal{N}(\mathbf{x}_i | \hat{\mathbf{x}}_i, \hat{\Sigma})$  for  $i = 1, \dots, n_{b-1}$ .
8     Set  $\tilde{\pi}_1(\mathbf{x}_i)$  to  $\mathcal{N}(\mathbf{x}_i | \mathbf{0}, \Lambda)$  for  $i = n_{b-1} + 1, \dots, n_b$ .
9      $\{\mathbf{s}_{0,k}\}_{k=1}^K \leftarrow \text{Particle\_Initialization}(\mathbf{D}^{(0)}, \mathbf{D}, \tilde{\pi}_0(\mathbf{X}), \tilde{\pi}_1(\mathbf{X}), \pi(\theta), K)$ 
10     $\{(s_{R,k}, W_{R,k})\}_{k=1}^K, \hat{Z}_R \leftarrow \text{Annealed\_SMC}(\{\mathbf{s}_{0,k}\}_{k=1}^K, \tilde{\pi}_0(\mathbf{X}), \tilde{\pi}_1(\mathbf{X}), \pi(\theta), l(\mathbf{D}|\mathbf{s}), \phi, \epsilon)$ 
11    Posterior approximation:  $\hat{\pi}(\mathbf{s}^{(b)}) = \sum_{k=1}^K W_{R,k} \times \delta_{\mathbf{s}_{R,k}}(\mathbf{s})$ .
12    Compute the weighted mean  $\hat{\mathbf{x}}_i$  and covariance  $\hat{\Sigma}$ ,  $i = 1, \dots, n_b$  from  $\{(s_{R,k}, W_{R,k})\}_{k=1}^K$ .
13    Reset  $\mathbf{D}^{(0)} \leftarrow \mathbf{D}$ .
```

---

## 4 Simulation Studies

We established the values for the prior parameters by utilizing empirical Bayes methods, following the recommendations outlined in [Oh and Raftery \(2001\)](#). For the prior of  $\sigma^2$ , we chose  $a = 5$  and  $b = SSR/m$  obtained from CMDS. For the prior of  $\psi$ , we chose  $c = -2$  and  $d = 2$ . For the hyperprior of  $\lambda_k$ , we set  $\alpha = 1/2$  and  $\beta_k = \frac{1}{2}s_k^{(0)}/n$ , where  $s_k^{(0)}/n$  is the sample variance of the  $k$ th coordinate of  $\mathbf{X}$  from CMDS. For the mixing distribution of  $\zeta_{i,j}$ , we used degrees of freedom  $\nu = 5$ . These parameter values deliver satisfactory results in the simulation studies, and the same values of the prior parameters are used in all examples unless otherwise specified.

In the Metropolis-Hastings algorithm, the multiplicity constant of the variance of the Gaussian proposal density for generating  $\mathbf{x}_i$  and  $\sigma^2$  is chosen based on the characteristics of the data to ensure rapid mixing. Since the number of significant attributes  $p$  is often unknown, most examples use  $p = 2$  for the purpose of visualization. In the annealed SMC algorithm, we set the number of particles to  $K = 200$ , the rCESS threshold to  $\phi = 0.8$ , and the resampling threshold to  $\epsilon = 0.5$ .

The primary objective of this simulation study is to evaluate the performance of various models under diverse data structures. We compared several candidate models, denoted as  $\mathcal{M}_g^{\mathcal{D}}$ , where  $g$  represents the model distribution for dissimilarities and  $\mathcal{D}$  is the dissimilarity metric used during estimation. We examined two experimental settings, one with skewed errors and the other with outliers. We present the outcomes from 20 runs with different random seeds.

## 4.1 Experiment 1: Data with skewed errors

We started by testing how the proposed model performs when data skewness is present. A detailed description of the data generation process with skewed errors is given in *Supplementary*. We simulated the accurate/unobserved observations  $\mathbf{X}$  from a combination of Gaussian distributions. Next, the noisy/observed observations  $\mathbf{Z}$  were generated through a two-step process. First, we introduced minor errors into all observations  $\mathbf{X}$  with the aim of simulating the systematic errors arising from data measurement. Second, varied percentages of the observations are subject to the contamination of moderate and significant errors, with the intention of replicating the scenario in which some observations are inaccurately recorded during data measurement. Specifically, moderate and significant errors were introduced into 20% and 2% of the observations, respectively. The Euclidean metric was then applied to obtain the dissimilarities  $d_{i,j}$ 's from the noisy observations  $\mathbf{Z}$  and the dissimilarities  $\tilde{d}_{i,j}$ 's from accurate observations  $\mathbf{X}$ . The errors  $\epsilon_{i,j}$ 's were computed by:

$$\epsilon_{i,j} = d_{i,j} - \tilde{d}_{i,j}, \quad i \neq j, i, j = 1, \dots, n.$$

A histogram of the errors  $\epsilon_{i,j}$ 's from one run is shown in Figure 2a. Our goal is to compare the performance of the proposed model  $\mathcal{M}_{TSN}^{\text{Euclidean}}$  with the standard model with truncated Gaussian  $\mathcal{M}_{TN}^{\text{Euclidean}}$  using the log marginal likelihoods when data are contaminated by some skewed errors.

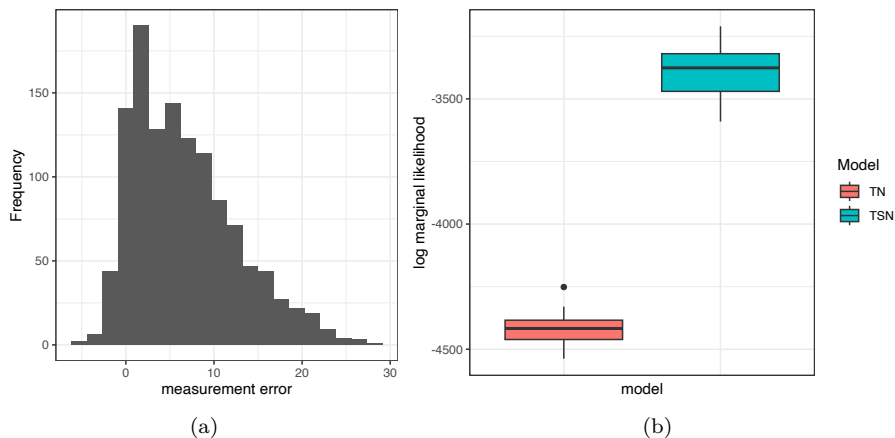


Figure 2: (a) Histogram of the errors. (b) The boxplots of the log marginal likelihood for different cases and models.

Figure 2b shows the performance comparison in terms of the log marginal likelihood as the skewed error presents. The findings of the study demonstrate that the model incorporating a truncated skewed Gaussian exhibits better performance, as the data under consideration is primarily with skewed errors. The results provide evidence that the skewed distributions are necessary for certain circumstances for modeling purposes.

## 4.2 Experiment 2: Data with outliers

In the following experiment, we used the wine dataset (Dua and Graff, 2017) to investigate the robustness of the proposed models. The wine dataset is obtained from a chemical analysis of wines planted in the same region in Italy but derived from different cultivars. The data contain 129 observations of wines with 13 constituents found in each wine. From the preliminary analysis of the wine types, 10 observations are labelled as outliers. We first calculated the Euclidean dissimilarities from the raw observations. To study the robustness of different models, we added more outliers by randomly selecting a different proportion of the dissimilarities and quadrupling their values. We considered two scenarios with varying proportions of outliers in dissimilarities; the first contains 10% outliers, and the second has 20% outliers.

Figure 3(a) shows the histograms of the dissimilarity  $d_{i,j}$ 's under the two scenarios. In scenario 2, the increased percentage of outliers leads to a heavier tail in the dissimilarity histogram. In this simulation, we assume the shape parameter  $\psi = 0$  to simplify the truncated skewed Gaussian to the standard truncated Gaussian. We test the robustness of the models  $\mathcal{M}_{TN}^{\text{Euclidean}}$  and  $\mathcal{M}_T^{\text{Euclidean}}$  in both scenarios.

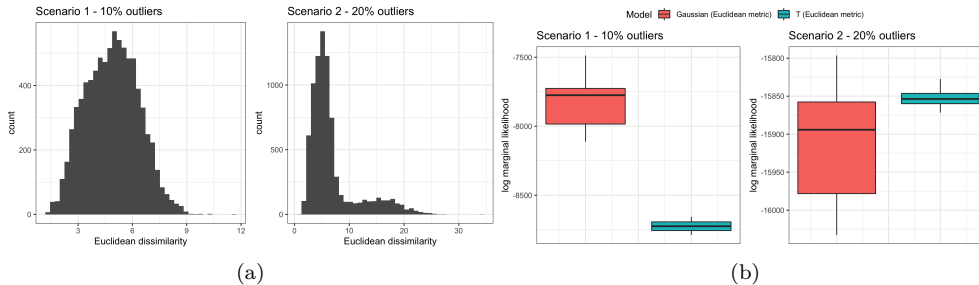


Figure 3: (a) The histograms of the dissimilarity  $d_{i,j}$  under Euclidean metrics. The left histogram is from scenario 1, where the data contain 10% outliers. The right histogram is from scenario 2, where the data contain 20% outliers. (b) The boxplots of the log marginal likelihood for different models. Red:  $\mathcal{M}_{TN}^{\text{Euclidean}}$ . Blue:  $\mathcal{M}_T^{\text{Euclidean}}$ . Dimension  $p$  is 2.

Figure 3(b) shows the marginal likelihood in log scale for the two models under the two scenarios. In scenario 1, where the data only contained 10% outliers, the histogram of the dissimilarity does not show a heavy tail. According to the left boxplot in Figure 3(b), the model  $\mathcal{M}_{TN}^{\text{Euclidean}}$  is preferred since it produces higher log marginal likelihoods overall. When the percentage of outliers is increased to 20%, an obvious heavier tail can be observed in the right histogram in Figure 3(a). This indicates fitting a more robust model  $\mathcal{M}_T^{\text{Euclidean}}$  is favored. We also find that the model  $\mathcal{M}_T^{\text{Euclidean}}$  produces smaller variances across seeds in both scenarios.

## 5 Data Applications

### 5.1 NIPS text data with incremental dimensions

In the first example, we demonstrate the performances of the adaptive inference with annealed SMC algorithm on some text data with incremental dimensions. The text data is generated from some real articles from Conference on Neural Information Processing Systems (NIPS). The NIPS dataset contains NIPS conference papers published between 1987 and 2015 (Dua and Graff, 2017; Perrone et al., 2017). In this study, our focus is directed toward a subset of the NIPS dataset, comprising a matrix of word counts extracted from 55 articles. This matrix is referred to as the document-term matrix, which is constructed after tokenization, removing stop words and truncation of the corpus by only keeping words appearing more than fifty times. The document-term matrix has counts for a list of 15005 words. Instead of Euclidean dissimilarity, we consider Cosine dissimilarity, which is suitable for discrete data such as word counts since it measures how dissimilar the documents are irrespective of their sizes.

We fitted the model  $\mathcal{M}_T^{\text{Cosine}}$  and compared the results in terms of STRESS values and computational times. The number of significant attributes  $p$  is assumed to be 2. In this toy example, we considered the cases with  $n_0 = 10, 50$ , and  $n_1 = 1, 5$ . For each combination of  $n_0$  and  $n_1$ , we looked at two cases: one uses the annealed SMC algorithm of fixed dimension on the  $n = n_0 + n_1$  observations with 100 particles, while the other uses the annealed SMC algorithm of incremental dimension with 50 particles given that the results from  $n_0$  observations are already known. In the second case, we can achieve similar results using a small set of particles since we have borrowed information from the estimation with  $n_0$  observations. From Table 1, it can be seen that the STRESS values from both cases are close, and this validates the performances of the annealed SMC algorithm for incremental dimension. For the two cases with  $n_0 = 10$ , the computation times had decreased by an average of 55% when applying the annealed SMC algorithm for incremental dimension. For the two cases with  $n_0 = 50$ , the computation times fall by 50% when applying the adaptive inference.

Observations	STRESS	Time (in sec)	Observations	STRESS	Time (in sec)
n = 11	0.8764	18.4	n = 51	0.7837	608.1
$n_0 = 10, n_1 = 1$	0.8568	8.3	$n_0 = 50, n_1 = 1$	0.7734	318.4
n = 15	0.8128	31.6	n = 55	0.8003	697.3
$n_0 = 10, n_1 = 5$	0.7842	13.7	$n_0 = 50, n_1 = 5$	0.8036	328.4

Table 1: A summary of the STRESS values and computation times from applying the annealed SMC on GBMDS to observations with different dimensions. The first and third rows present the results from applying the annealed SMC algorithm of fixed dimension to all observations. The results in the second and fourth rows come from running the annealed SMC algorithm of incremental dimension, given the results from  $n$  observations are known. All results are the averages of 20 runs.

## 5.2 Geographical data

The second example aims to study the performance of the proposed method and present visualizations of the estimations with uncertainty measures. As an illustrative example to study the performances of the CMDS and BMDS methods, we considered the US cities dataset from the US Census Bureau (Census Bureau, 2021), which contains Latitude and Longitude information from 15 large US cities. To evaluate the performances of the GBMDS, we appended 10 noise variables to add complexity. These noise variables are generated from a Gaussian distribution with a mean of 0 and variance comparable to the “Latitude” or “Longitude” variables.

We performed experiments across three scenarios, each of which had a distinct set of noises added to the data. The noises are incorporated into the data by assigning varying weights to the true and noisy variables. We represent the signal-to-noise ratio as  $R_{s:n}$ , which is defined as the ratio of the weight of the true signal to that of the noise. If  $R_{s:n} > 1$ , it indicates that there is more signal than noise. In the first scenario, we assigned equal importance to all variables, resulting in  $R_{s:n} = 1$ . In this case, the results depend equally on the signal and noisy variables. In the second scenario, we placed more emphasis on crucial variables such as “Latitude” and “Longitude” by decreasing the weights assigned to redundant noises, setting  $R_{s:n} = 4$ . In the third scenario, we tested an extreme condition where the majority of the weights were allocated to the “Latitude” and “Longitude” variables, setting  $R_{s:n} = 10$ . In all experiments, we normalized the weights to ensure they sum up to 1.

We employed two Bayesian methods, MCMC and annealed SMC (ASMC), to implement our proposed GBMDS. To initialize the GBMDS, we utilized the results from CMDS. For simplicity, we assumed  $\psi = 0$  to reduce the model to  $\mathcal{M}_{TN}^{\text{Euclidean}}$ . To ensure a fair comparison between the two Bayesian methods, we kept the computational budget constant. Specifically, we first ran annealed SMC with 300 particles and recorded the number of iterations. We then allocated the same budget to MCMC by setting the number of MCMC iterations equal to the product of the annealed SMC iterations and the number of particles.

Table 2 presents the STRESS values obtained from CMDS, GBMDS with MCMC (GBMDS-MCMC), and GBMDS with ASMC (GBMDS-ASMC) for the three scenarios. Our analysis indicates that Bayesian approaches yield lower STRESS values across all three scenarios. Furthermore, we observed that annealed SMC outperformed MCMC in terms of generating smaller STRESS values under the same computational budget in Scenarios 2 and 3. It is interesting to discover that the better performance of annealed SMC is more pronounced when the signal-to-noise ratios are high.

	CMDS	GBMDS-MCMC	GBMDS-ASMC
Scenario 1: $R_{s:n} = 1$	0.4557	<b>0.3231</b>	0.3521
Scenario 2: $R_{s:n} = 4$	0.4680	0.4327	<b>0.3910</b>
Scenario 3: $R_{s:n} = 10$	0.4726	0.4414	<b>0.4103</b>

Table 2: A Summary of the STRESS values for different methods on US City data under scenarios 1 to 3 with different noise-to-signal ratios.

Figure 4 displays the estimated locations of the 15 US cities obtained by GBMDS-ASMC. Some transformations, such as rotation and reflection, were applied to the estimated locations from GBMDS-ASMC to fit the cities' actual geographical locations. One can observe from Figures 4(a) and 4(d) that under the equal weight scenario, several cities are geographically misplaced no matter what transformations are applied. The reason behind this mismatch is that the information in the "Latitude" and "Longitude" variables are masked by the remaining variables. The estimated locations shown in 4(c) and 4(f) lead to a closer match when higher weights are assigned to the "Latitude" and "Longitude" variables.

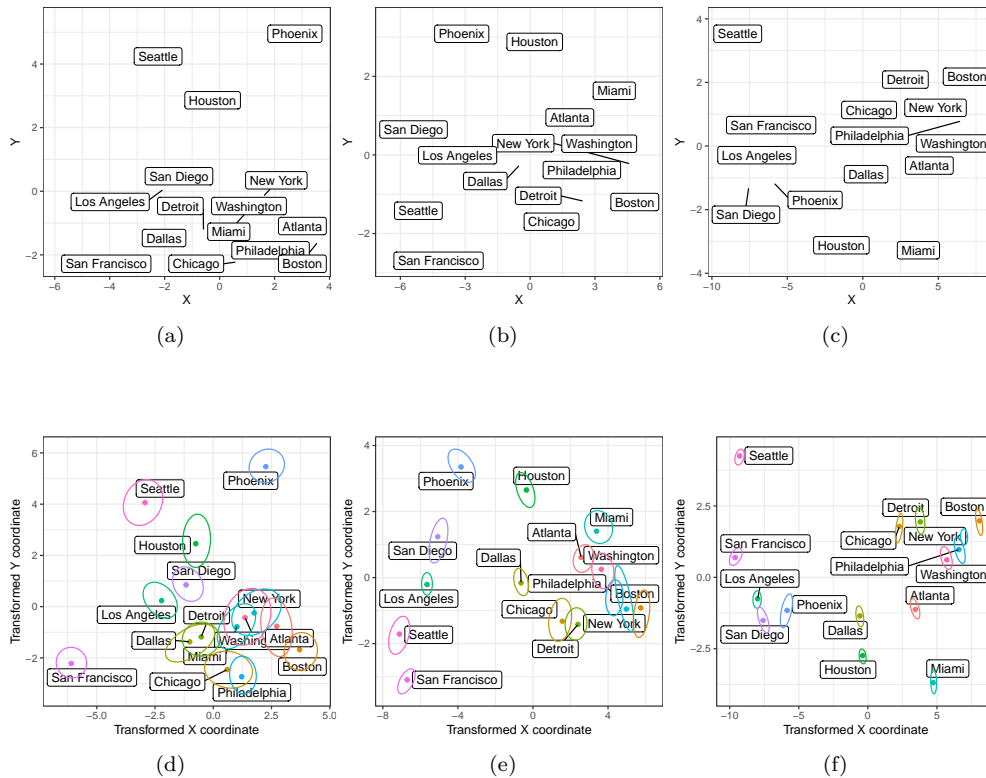


Figure 4: Estimated locations of the 15 US cities from CMDS and GBMDS-ASMC after transformations. Sub-figures (a) to (c) are results from CMDS and (d) to (f) are from GBMDS-ASMC.  $R_{s:n} = 1$  in (a) and (d),  $R_{s:n} = 4$  in (b) and (e),  $R_{s:n} = 10$  in (c) and (f). For GBMDS-ASMC, the ellipses are generated from all the posterior samples with the 95% credible regions. The posterior medians of  $\mathbf{x}_i$ 's are served as the estimated coordinates of the 15 US cities in the two-dimensional space.

The Bayesian approach offers several advantages over the classical approach. In addition to producing smaller STRESS values, the Bayesian approach enables the estimation of uncertainty by leveraging samples from the posterior distribution. To this

end, we performed Procrustes transformations on the posterior samples of  $\mathbf{x}_i$  to align each sample as closely as possible to the estimated coordinates, effectively standardizing all the posterior samples of  $\mathbf{x}_i$ . Using the transformed posterior samples, we constructed credible regions, represented as ellipses in Figures 4(d) to 4(f). In contrast to CMDS, our GBMDS-ASMC method offers uncertainty measures, with tight credible regions in scenarios where the signal-to-noise ratio is high and wider credible regions when more noises exist in the data.

### 5.3 NIH text data

In this example, we applied the MDS techniques to text data consisting of documents and words. Our aim was to showcase the application of our proposed method and investigate the effect of dimension  $p$ . The dataset holds information on research grants awarded by the National Institutes of Health (NIH) in 2014 (Jones, 2021). The raw data contain 100 randomly-sampled grant abstracts and metadata. To preprocess the data, we performed tokenization and removed stop words. This results in a document-term matrix with a dimension of 23915 by 100, where each column represents an abstract and contains the word counts for all words in that abstract. We then re-weighted the word counts by multiplying an inverse document frequency vector to adjust for the relative importance of words in the entire collection of documents. The purpose of this reweighing step was to account for the varying frequencies of words across documents.

We calculated the Cosine dissimilarities of the documents and used them as input to the MDS methods. We varied the dimension  $p$  from 2 to 6 to investigate its effect on the results. Table 3 displays a comparison of CMDS and GBMDS-ASMC using STRESS. For GBMDS-ASMC, we tested four candidate models, and the optimal model (indicated in bold) was selected based on the log marginal likelihood estimates for each dimension. The results indicate that GBMDS-ASMC provides a better representation of the data in lower-dimensional space, with smaller STRESS values than CMDS. Moreover, the optimal model chosen by the log marginal likelihood estimate is consistent with the model with the smallest STRESS value for  $p > 3$ . For  $p = 2, 3$ , the optimal models selected by the log marginal likelihood estimates have the third and second smallest STRESS values, respectively.

Model		Dimension				
		2	3	4	5	6
CMDS		0.8493	0.8171	0.7892	0.7598	0.7335
GBMDS-ASMC	$\mathcal{M}_T^{\text{Euclidean}}$	<b>0.7558</b>	<b>0.6599</b>	0.6571	0.6057	0.5609
	$\mathcal{M}_T^{\text{Cosine}}$	0.7715	0.6901	0.6503	0.6357	0.5720
	$\mathcal{M}_{TSN}^{\text{Euclidean}}$	0.4921	0.4343	<b>0.3942</b>	<b>0.3804</b>	<b>0.3499</b>
	$\mathcal{M}_{TSN}^{\text{Cosine}}$	0.7024	0.6671	0.6152	0.5974	0.5634

Table 3: A summary of the STRESS values from applying the different MDS methods on the text data. For the GBMDS-ASMC method, the STRESS value in bold is the optimal model selected by the largest log marginal likelihood estimates in a given dimension.



## 6 Conclusion

In this work, we developed multiple ways to model the dissimilarity measures for multi-dimensional scaling, proposed a general adaptive annealed SMC algorithm for Bayesian inference, and applied the model selection via marginal likelihoods. We considered the problem of adaptive inferences with annealed SMC algorithm for an increasing dimension of the observations and parameters. The simulation results demonstrate a significant reduction in computational time while maintaining comparable accuracy when compared to the annealed SMC with a fixed dimension. We leveraged the rich MCMC literature on classical Metropolis-Hastings moves as the basis of proposal distributions in the adaptive annealed SMC. Moreover, the adaptive annealed SMC algorithm is easy to parallelize for batches of particles, which explicitly takes advantage of parallel processors' capabilities and boosts computing. Both the simulations and real data applications demonstrate the accuracy and effectiveness of the proposed adaptive annealed SMC algorithm for dimension reduction and model comparison.

On the basis of the GBMDS estimates of object configuration over various models and a range of dimensions  $p$ , we proposed to use the marginal likelihood to choose the optimal combination. Compared with choosing dimensions by a simple Bayesian criterion in [Oh and Raftery \(2001\)](#), our fully Bayesian approach can incorporate prior comparison and directly utilize the unbiased marginal likelihood estimator from the annealed SMC algorithm for the choice of model and dimension. In contrast to the frequentist model selection via STRESS, which generally relies on the specifically-constructed statistics applicable to particular cases, Bayesian model selection has the simplicity of a maximum likelihood method regardless of the data or model being used as well as the advantage of penalizing more complex models. Furthermore, we obtained the marginal likelihood estimate as a byproduct of sampling from the algorithm. This efficient method of estimating the marginal likelihood from the annealed SMC lays the foundation for comparing MDS models with different metrics and dimensions. This also gives a notable computational advantage of the proposed annealed SMC over the existing MCMC-based methods.

We have implemented the Procrustes transformations on the posterior samples to deal with the non-identifiability issue. The transformed posterior samples are used to construct the credible regions to display uncertainty measures. In the geographical data example, we noted that the credible regions for some observations are relatively broad, indicating that one should interpret specific patterns with care. Other appropriate transformations to post-process the posterior samples can be considered to improve the interpretability. In addition, it would be interesting to investigate the influence of the number of particles in the annealed SMC algorithm on the credible regions.

One application of MDS is to visualize objects in a reduced dimensional space. Our proposed framework can help find a good model for the dissimilarities and an optimal  $p$  for the dimension reduction. Typically, the visualization works better for the model with the Euclidean metric in a two-dimensional space. It is beyond the scope of this study to investigate the possible visualizations for the optimal  $p$ -dimensional space with a non-Euclidean metric. This will be left for exploration in future work.

Another interesting application of MDS is to cluster objects, where similar observations are grouped into clusters based on dissimilarity. With MDS techniques, we can

obtain the coordinates of objects in a low-dimensional space. Visual display of clusters in a low-dimensional space is of interest since it may provide helpful information about the relationship between the groups and the underlying data generation process. Model-based clustering with dissimilarities was proposed by [Oh and Raftery \(2007\)](#), and the resulting model is estimated in a Bayesian way using MCMC. One can modify the adaptive annealed SMC algorithm to perform MDS and model-based clustering simultaneously. This model-based clustering algorithm also applies to text clustering when appropriate metrics are used to describe dissimilarities between texts. Moreover, in this study, we have explored the sequential estimation of object configuration using the adaptive annealed SMC algorithm. To enhance the computational efficiency of a single run of the annealed SMC algorithm outlined in [Algorithm 2](#), one can consider implementing the resampling method as seen in [Gunawan et al. \(2020\)](#) or employ more intricate approaches for parallelization. These strategies can enable the scalability of the proposed method to accommodate datasets with substantial sample sizes.

## Supplementary Material

Supplementary Materials to “Generalized Bayesian Multidimensional Scaling and Model Comparison”. Supplementary materials include (i) a document with the details of the dissimilarity metrics, likelihood function derivation, details of the particle propagation step, and details of the data-generating process in simulation studies. (ii) R code which implements the proposed model and some demos from [Sections 4 and 5](#).

## References

- Bakker, R. and Poole, K. T. (2013). “Bayesian metric multidimensional scaling.” *Political Analysis*, 21(1): 125–140. [2](#)
- Berger, J. O., Pericchi, L. R., Ghosh, J., Samanta, T., De Santis, F., Berger, J., and Pericchi, L. (2001). “Objective Bayesian methods for model selection: Introduction and comparison.” *Lecture Notes-Monograph Series*, 135–207. [10](#)
- Berk, R. H. (1966). “Limiting behavior of posterior distributions when the model is incorrect.” *The Annals of Mathematical Statistics*, 37(1): 51–58. [10](#)
- Borg, I. and Groenen, P. J. (2005). *Modern multidimensional scaling: Theory and applications*. Springer Science & Business Media. [2](#)
- Bronstein, A. M., Bronstein, M. M., and Kimmel, R. (2006). “Generalized multidimensional scaling: a framework for isometry-invariant partial surface matching.” *Proceedings of the National Academy of Sciences*, 103(5): 1168–1172. [3](#)
- Census Bureau, U. S. (2021). “United States Census Bureau: Data & Map.” URL <https://www.census.gov/data.html> [22](#)
- Chib, S. and Jeliazkov, I. (2001). “Marginal likelihood from the Metropolis–Hastings output.” *Journal of the American Statistical Association*, 96(453): 270–281. [10](#)

- Del Moral, P. (2004). *Feynman-Kac Formulae*. Springer. 14
- Del Moral, P., Doucet, A., and Jasra, A. (2006). “Sequential Monte Carlo samplers.” *Journal of the Royal Statistical Society: Series B (Statistical Methodology)*, 68(3): 411–436. 3, 11, 12, 14
- (2007). “Sequential Monte Carlo for Bayesian Computation.” *Bayesian Statistics*, 8: 1–34. 11
- (2012). “An adaptive sequential Monte Carlo method for approximate Bayesian computation.” *Statistics and Computing*, 22: 1009–1020. 3
- Douc, R. and Cappé, O. (2005). “Comparison of resampling schemes for particle filtering.” In *ISPA 2005. Proceedings of the 4th International Symposium on Image and Signal Processing and Analysis, 2005.*, 64–69. IEEE. 14
- Doucet, A., Briers, M., and Sénécal, S. (2006). “Efficient block sampling strategies for sequential Monte Carlo methods.” *Journal of Computational and Graphical Statistics*, 15(3): 693–711. 3
- Doucet, A., De Freitas, N., Gordon, N. J., et al. (2001). *Sequential Monte Carlo methods in practice*, volume 1. Springer. 3
- Doucet, A. and Johansen, A. M. (2009). “A tutorial on particle filtering and smoothing: Fifteen years later.” *Handbook of Nonlinear Filtering*, 12(656-704): 3. 3, 14
- Dua, D. and Graff, C. (2017). “UCI Machine Learning Repository.” URL <http://archive.ics.uci.edu/ml> 20, 21
- Fan, Y., Wu, R., Chen, M.-H., Kuo, L., and Lewis, P. O. (2011). “Choosing among partition models in Bayesian phylogenetics.” *Molecular Biology and Evolution*, 28(1): 523–532. 11
- Goodall, C. (1991). “Procrustes methods in the statistical analysis of shape.” *Journal of the Royal Statistical Society: Series B (Methodological)*, 53(2): 285–321. 11
- Gronau, Q. F. and Lee, M. D. (2020). “Bayesian inference for multidimensional scaling representations with psychologically interpretable Metrics.” *Computational Brain & Behavior*, 3(3): 322–340. 2
- Gunawan, D., Dang, K.-D., Quiroz, M., Kohn, R., and Tran, M.-N. (2020). “Subsampling sequential Monte Carlo for static Bayesian models.” *Statistics and Computing*, 30(6): 1741–1758. 26
- Han, C. and Carlin, B. P. (2001). “Markov chain Monte Carlo methods for computing Bayes factors: A comparative review.” *Journal of the American Statistical Association*, 96(455): 1122–1132. 3
- Holbrook, A. J., Lemey, P., Baele, G., Dellicour, S., Brockmann, D., Rambaut, A., and Suchard, M. A. (2020). “Massive parallelization boosts big Bayesian multidimensional scaling.” *Journal of Computational and Graphical Statistics*, 1–14. 2
- Jeffreys, H. (1935). “Some tests of significance, treated by the theory of probability.” In

- Mathematical Proceedings of the Cambridge Philosophical Society*, volume 31, 203–222. Cambridge University Press. 3
- Jones, T. (2021). *textmineR: Functions for text mining and topic modeling*. R package version 3.0.5.  
URL <https://CRAN.R-project.org/package=textmineR> 24
- Kass, R. E. and Raftery, A. E. (1995). “Bayes factors.” *Journal of the American Statistical Association*, 90(430): 773–795. 10
- Kong, A. (1992). “A note on importance sampling using standardized weights.” *University of Chicago, Dept. of Statistics, Tech. Rep.*, 348. 14
- Kruskal, J. B. (1964). “Multidimensional scaling by optimizing goodness of fit to a nonmetric hypothesis.” *Psychometrika*, 29(1): 1–27. 10
- Lange, K. L., Little, R. J., and Taylor, J. M. (1989). “Robust statistical modeling using the t distribution.” *Journal of the American Statistical Association*, 84(408): 881–896. 7
- Li, B. and Han, L. (2013). “Distance weighted Cosine similarity measure for text classification.” In *International Conference on Intelligent Data Engineering and Automated Learning*, 611–618. Springer. 3
- Lin, L. and Fong, D. K. (2019). “Bayesian multidimensional scaling procedure with variable selection.” *Computational Statistics & Data Analysis*, 129: 1–13. 2, 7
- Mémoli, F. (2011). “Gromov–Wasserstein distances and the metric approach to object matching.” *Foundations of Computational Mathematics*, 11(4): 417–487. 3
- Neal, R. M. (2001). “Annealed importance sampling.” *Statistics and Computing*, 11(2): 125–139. 11
- Neal, R. M. et al. (2011). “MCMC using Hamiltonian dynamics.” *Handbook of Markov chain Monte Carlo*, 2(11): 2. 2
- Oh, M.-S. and Raftery, A. E. (2001). “Bayesian multidimensional scaling and choice of dimension.” *Journal of the American Statistical Association*, 96(455): 1031–1044. 2, 5, 6, 14, 18, 25
- (2007). “Model-based clustering with dissimilarities: A Bayesian approach.” *Journal of Computational and Graphical Statistics*, 16(3): 559–585. 2, 26
- Perrone, V., Jenkins, P. A., Spano, D., and Teh, Y. W. (2017). “Poisson random fields for dynamic feature models.” *Journal of Machine Learning Research*, 18. 21
- Robert, C. P. and Wraith, D. (2009). “Computational methods for Bayesian model choice.” In *AIP Conference Proceedings*, volume 1193, 251–262. American Institute of Physics. 10
- Robert, C. P. et al. (2007). *The Bayesian choice: from decision-theoretic foundations to computational implementation*, volume 2. Springer. 10

- Skilling, J. (2004). “Nested sampling.” In *AIP Conference Proceedings*, volume 735, 395–405. American Institute of Physics. [10](#)
- Torgerson, W. S. (1952). “Multidimensional scaling: I. Theory and method.” *Psychometrika*, 17(4): 401–419. [2](#), [5](#)
- Wang, L., Wang, S., and Bouchard-Côté, A. (2020). “An annealed sequential Monte Carlo method for Bayesian phylogenetics.” *Systematic Biology*, 69(1): 155–183. [3](#), [10](#), [11](#), [16](#)
- Wang, S., Ge, S., Doig, R., and Wang, L. (2021). “Adaptive semiparametric Bayesian differential equations via sequential Monte Carlo.” *Journal of Computational and Graphical Statistics*, 1–14. [3](#)
- Zhou, Y., Johansen, A. M., and Aston, J. A. (2016). “Toward automatic model comparison: an adaptive sequential Monte Carlo approach.” *Journal of Computational and Graphical Statistics*, 25(3): 701–726. [3](#), [16](#)

# Supplementary Materials to “Generalized Bayesian Multidimensional Scaling and Model Comparison”

## 1 Distance (Dissimilarity) Metric

In this section, we will formally define the metric space and introduce several dissimilarity metrics that are used in the paper. Let  $M$  be a set and let  $\mathcal{D}$  be a real-valued function defined on the Cartesian product  $M \times M$  satisfying:

1.  $\mathcal{D}(x, y) \geq 0, \forall x, y \in M$ ;
2.  $\mathcal{D}(x, y) = 0 \iff x = y$ ;
3.  $\mathcal{D}(x, y) = \mathcal{D}(y, x), \forall x, y \in M$ ;
4.  $\mathcal{D}(x, z) \leq \mathcal{D}(x, y) + \mathcal{D}(y, z), \forall x, y, z \in M$ .

Then the function  $\mathcal{D}$  is considered as a metric or dissimilarity function in  $M$ , and the set  $M$  together with  $\mathcal{D}$  is called a metric space. We will denote a vector in  $\mathbb{R}^q$  in bold when  $q > 1$  and refer to its scalar components by subscripts. For instance, let  $\mathbf{x} \in \mathbb{R}^q$  be a vector with  $\mathbf{x} = (x_1, \dots, x_q)^\top$  representing the values of  $q$  attributes. We consider the following dissimilarity metrics on  $\mathbb{R}^q$ :

- Euclidean metric ( $L^2$  norm):  $\mathcal{D}(\mathbf{x}, \mathbf{y}) = \|\mathbf{x} - \mathbf{y}\|_2 = \sqrt{\sum_{i=1}^q (x_i - y_i)^2}$
- Cosine metric:  $\mathcal{D}(\mathbf{x}, \mathbf{y}) = 1 - (\sum_{i=1}^q x_i y_i) / (\sqrt{\sum_{i=1}^q x_i^2} \sqrt{\sum_{i=1}^q y_i^2})$  (The Cosine metric is used in the case of text analysis, as word frequencies are non-negative, the Cosine metric ranges from 0 to 1.)

The present work exclusively incorporates the Euclidean and Cosine metrics. Nonetheless, the proposed methods have the potential for application across a broader range of dissimilarity metrics.

## 2 Derivation of the Likelihood Function of the Unknown Parameters under Model $\mathcal{M}_T$

$$\begin{aligned}
 l(\{\mathbf{x}_{1:n}\}, \sigma^2, \zeta \mid \mathbf{D}, \mathcal{M}_T) &= \prod_{i>j} \frac{1}{\sqrt{2\pi\sigma^2/\zeta_{i,j}}} \times \exp\left\{-\frac{(d_{i,j} - \delta_{i,j})^2}{2\sigma^2/\zeta_{i,j}}\right\} \\
 &\quad \times \left\{1 - \Phi\left(-\frac{\delta_{i,j}}{\sigma/\zeta_{i,j}}\right)\right\}^{-1} \\
 &= (2\pi\sigma^2)^{-\frac{m}{2}} \times \exp\left\{\frac{1}{2} \sum_{i>j} \log(\zeta_{i,j}) - \frac{1}{2\sigma^2} \sum_{i>j} \zeta_{i,j} (d_{i,j} - \delta_{i,j})^2\right\}
 \end{aligned}$$

$$\left. - \sum_{i>j} \log \Phi \left( \frac{\delta_{i,j} \sqrt{\zeta_{i,j}}}{\sigma} \right) \right\}$$

### 3 Conditional posterior distributions in the particle propagation step

In this section, we describe the conditional posterior distributions for the parameters. In each conditional posterior distribution, we use  $|\cdots$  to denote conditioning on the data and all other parameters and/or indicators.

- The full conditional distribution for  $\lambda_k$  is

$$\lambda_k | \cdots \sim IG(\alpha + n/2, \beta_k + \tau_r s_k/2), \quad (1)$$

where  $s_k/n$  is the sample variance of the  $k$ th coordinates of  $\mathbf{x}_i$ 's

- The full conditional posterior distributions of  $\{\mathbf{x}_{1:n}\}$  and  $\sigma^2$  are

$$\begin{aligned} \gamma_r(\{\mathbf{x}_{1:n}\} | \cdots, \mathcal{M}_{TSN}) \propto \exp \left\{ -\tau_r \left( \frac{1}{2\sigma^2} \text{SSR} + \frac{m}{2} \log \left( \sigma^2 (1 - F_{\delta_{i,j}, \sigma, \psi}(0)) \right) \right) \right. \\ \left. - \sum_{i>j} \log \left( \Phi \left( \psi \frac{d_{i,j} - \delta_{i,j}}{\sigma} \right) \right) + \frac{1}{2} \sum_{i=1}^n \mathbf{x}_i^\top \Lambda^{-1} \mathbf{x}_i \right\}, \end{aligned} \quad (2)$$

$$\begin{aligned} \gamma_r(\{\mathbf{x}_{1:n}\} | \cdots, \mathcal{M}_T) \propto \exp \left\{ -\tau_r \left( \frac{1}{2\sigma^2} \sum_{i>j} \zeta_{i,j} (d_{i,j} - \delta_{i,j})^2 \right) \right. \\ \left. + \sum_{i>j} \log \Phi \left( \frac{\delta_{i,j} \sqrt{\zeta_{i,j}}}{\sigma} \right) + \frac{1}{2} \sum_{i=1}^n \mathbf{x}_i^\top \Lambda^{-1} \mathbf{x}_i \right\} \end{aligned} \quad (3)$$

where  $\text{SSR} = \sum_{i>j} (d_{i,j} - \delta_{i,j})^2$ ,  $F(\cdot)$  is the cdf of skewed Gaussian distribution,  $\Phi(\cdot)$  is the standard Gaussian cdf, and  $m = n(n-1)/2$  is the total number of dissimilarities for  $n$  objects.

$$\begin{aligned} \gamma_r(\sigma^2 | \cdots, \mathcal{M}_{TSN}) \propto \sigma^{-2(a+1)} \exp \left\{ -\tau_r \left( \frac{1}{2\sigma^2} \text{SSR} + \frac{m}{2} \log \left( \sigma^2 (1 - F_{\delta_{i,j}, \sigma, \psi}(0)) \right) \right) \right. \\ \left. - \sum_{i>j} \log \left( \Phi \left( \psi \frac{d_{i,j} - \delta_{i,j}}{\sigma} \right) \right) + \frac{b}{\sigma^2} \right\}, \end{aligned} \quad (4)$$

$$\begin{aligned} \gamma_r(\sigma^2 | \dots, \mathcal{M}_T) \propto \sigma^{-m} \exp \left\{ -\tau_r \left( \frac{1}{2\sigma^2} \sum_{i>j} \zeta_{i,j} (d_{i,j} - \delta_{i,j})^2 \right. \right. \\ \left. \left. + \sum_{i>j} \log \Phi \left( \frac{\delta_{i,j} \sqrt{\zeta_{i,j}}}{\sigma} \right) + \frac{b}{\sigma^2} \right) \right\} \end{aligned} \quad (5)$$

The full conditional posterior distributions of  $\{\mathbf{x}_{1:n}\}$  and  $\sigma^2$  do not admit closed forms, a random walk Metropolis-Hastings step is implemented with the Gaussian proposal densities. The full conditional posterior distribution of  $\psi$  also does not have a closed form. A random walk Metropolis-Hastings step with Gaussian proposal density is applied. At iteration  $r$ , we perform the following steps:

1. Propose new variates with Gaussian proposals:

$$\begin{aligned} \{\mathbf{x}_{1:n}\}_* &\sim N(\{\mathbf{x}_{1:n}\}_{r-1}, c\sigma_{r-1}^2/(n-1)), \\ \sigma_*^2 &\sim N(\sigma_{r-1}^2, \sigma_{r-1}^2), \\ \psi_* &\sim N(\psi_{r-1}, 0.1^2), \end{aligned}$$

where  $c$  is a constant multiplier and  $\sigma_{r-1}^2$  is the variance of  $IG(a+m/2, b+SSR/2)$  distribution.

2. Compute the Metropolis-Hastings Ratio:

$$r_{MH} = \min \left\{ 1, \frac{\gamma_r(\{\mathbf{x}_{1:n}\}_*, \sigma_*^2, \psi_* | \dots)}{\gamma_r(\{\mathbf{x}_{1:n}\}_{r-1}, \sigma_{r-1}^2, \psi_{r-1} | \dots)} \right\}$$

3. Generate  $u \sim \text{Uniform}(0, 1)$  distribution:

- If  $u \leq r_{MH}$ , then accept  $\{\mathbf{x}_{1:n}\}_*, \sigma_*^2, \psi_*$ . Set  $\{\mathbf{x}_{1:n}\}_r = \{\mathbf{x}_{1:n}\}_*, \sigma_r^2 = \sigma_*^2, \psi_r = \psi_*$ .
- If  $u > r_{MH}$ , then reject  $\{\mathbf{x}_{1:n}\}_*, \sigma_*^2, \psi_*$ . Set  $\{\mathbf{x}_{1:n}\}_r = \{\mathbf{x}_{1:n}\}_{r-1}, \sigma_r^2 = \sigma_{r-1}^2, \psi_r = \psi_{r-1}$ .

- For model  $\mathcal{M}_T$ , the full conditional distribution for  $\zeta_{i,j}$  is

$$\zeta_{i,j} | \dots, \mathcal{M}_T \sim \text{Gamma}((\tau_r + \nu)/2, \tau_r(d_{i,j} - \delta_{i,j})^2/(2\sigma^2) + \nu/4). \quad (6)$$

## 4 Data generation process for Skewed Measurement Errors

This section details the data-generating process for Experiment 1 in the simulation studies. We generated 50 accurate/unobserved observations  $\mathbf{X} = \{\mathbf{x}_1, \dots, \mathbf{x}_{50}\}$  of size 20. These accurate observations were simulated as a combination of 50% from  $\mathcal{N}(0, 1)$ , 25% from  $\mathcal{N}(100, 10)$  and 25% from  $\mathcal{N}(-10, 1)$ . The noisy/observed observations  $\mathbf{Z} = \{\mathbf{z}_1, \dots, \mathbf{z}_{50}\}$  were simulated by successively adding two types of artificial measurement errors to the accurate observations  $\mathbf{X}$ . First, we added some errors corresponding to



some systematic errors that occur during data measurement. For example, some measures are always higher than the actual values. We incorporated this information into the accurate observations by adding measurement errors simulated from  $\mathcal{N}(0, 1)$ . The second type of error reflects the nature that a few observations are mistakenly recorded and deviate from the truth by a significant amount. These observations are treated as outliers. Outliers are introduced using a Categorical random variable  $C_i \sim \text{Cat}(1, \mathbf{p})$ ,  $i = 1, \dots, 50$ ,  $\mathbf{p} = (p_1, p_2, 1 - p_1 - p_2)$ , with  $p_1$  and  $p_2$  corresponding to outliers' percentages. In the simulation, we studied the performance of the proposed model, and we set  $p_1 = 0.2$  and  $p_2 = 0.02$ . Observations were generated as follows:

- When  $C_i = 1$ , the observation is contaminated by moderate measurement error: measurement errors are generated from  $\mathcal{N}(10, 1)$  and added to the observation
- When  $C_i = 2$ , the observation is contaminated by large measurement error: measurement errors are generated from  $\mathcal{N}(20, 1)$  and added to the observation
- When  $C_i = 3$ , the observation is not contaminated

The Euclidean metric was then applied to obtain the dissimilarities  $d_{i,j}$ 's from the noisy observations  $\mathbf{Z} = \{\mathbf{z}_1, \dots, \mathbf{z}_{50}\}$  and the dissimilarities  $\tilde{d}_{i,j}$ 's from accurate measurements  $\mathbf{X} = \{\mathbf{x}_1, \dots, \mathbf{x}_{50}\}$ , respectively. The measurement errors  $\epsilon_{i,j}$ 's were computed by:

$$\epsilon_{i,j} = d_{i,j} - \tilde{d}_{i,j}, \quad i \neq j, \quad i, j = 1, \dots, n. \quad (1)$$

The histograms of  $d_{i,j}$ 's,  $\tilde{d}_{i,j}$ 's and  $\epsilon_{i,j}$ 's are displayed in Figure 1. We can see that the measurement errors do not necessarily follow the Gaussian distribution, and the distribution of the observed dissimilarities is skewed.

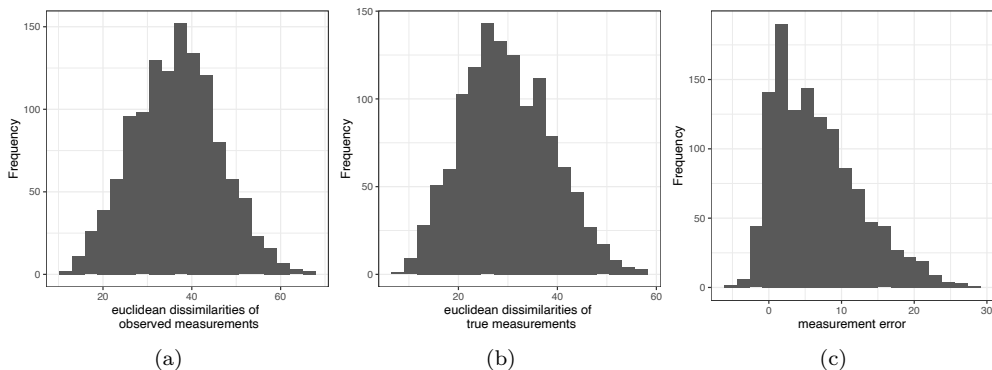


Figure 1: (a) Histogram of the observed dissimilarities  $d_{i,j}$ 's. (b) Histogram of the true dissimilarities  $\tilde{d}_{i,j}$ 's. (c) Histogram of the measurement errors  $\epsilon_{i,j}$ 's.